3D THROUGH THE WALL MICROWAVE IMAGING

By

Nimra Shafi

Beenish Noor

Usman Mirza

Muhammad Ali Chattha

Submitted to the Department of Electrical Engineering

National University of Sciences and Technology, Islamabad

in partial fulfillment for the requirements of a B.E Degree in

Telecommunication Engineering

AUGUST 2011

Abstract

Through the wall imaging, meaning capacity to look beyond the wall or visually opaque object has been of particular interest in modern era since situational awareness is of vital importance at numerous occasions especially in defense related operations. The capability of microwave signals to penetrate light opaque materials and sense distant or inaccessible objects with reasonable spatial resolution makes them attractive for detecting objects beyond the wall. Imaging through wall was initiated in Pakistan by the students of MCS last year. Keeping in view the considerable work done by them and being the need of the hour due to the environment prevailing in the country we decided to pursue it and enhance it to the next level.

The project builds on the concept of Synthetic Aperture Radar Beamforming [13]. The algorithm from previous project [2] takes large computational time; our algorithm has significantly reduced this time for 2 dimensional imaging of an object behind the wall. This substantial improvement in the algorithm has been achieved by a novel concept called "CUBISM". The concept of CUBISM has been extended in developing efficient algorithm for 3 dimensional imaging of an object giving information about its location in depth as well as in azimuth plane. The algorithm is implemented on a dedicated processor that will ensure portability at the software level.

The image obtained shows a 3D structure of the object in the target area. The dimensions of the obtained 3D image depict the true dimensions of the object in the target area and its exact location is also identified.

We humbly dedicate our work to the Lord of the worlds Whose knowledge extend over the heavens and the earth and to the Holy Prophet may peace and blessings be upon Him

ACKNOWLEDGEMENTS

We as a group are grateful to all those people who helped us in the completion of this project, especially to our supervisor Dr Naveed Iqbal Rao for being a torch bearer for us. His expertise in this field has always been a source of inspiration for us. We are grateful to him for providing us an opportunity to perform our BE final year project in his Image processing group. We are really thankful to his contributions in our project work.

We would like to specially thank and express our heartily gratitude to our Co-supervisor lecturer Mir Yasir Umair and Lec. Safwat Irteza Butt. It would have not been possible without their moral and technical support. We are grateful to Ms Zainab Tahir, Ms Amina Masood, NC Waqas Ahmed, NC Zubair, NC Mehreen Shahid and our families for their constant support in hard times, we can never forget that.

Table of Contents

LIST OF TABLES vii
LIST OF FIGURES viii
LIST OF SYMBOLS/ ABBREVIATIONS x
CHAPTER 1: OVERVIEW 1
1.1 Introduction 1
1.2 Problem statement 2
1.3 Scope/ objectives 2
1.4 Applications 3
CHAPTER 2: BACKGROUND 5
2.1 Introduction 5
2.2 Antenna specifications 6
2.3 VNA-LAN interface 8
2.4 Connecting/configuring the analyzer to LAN 8
2.5 LAN-FTP interface 9
2.6 2D Antenna Positioning Assembly 9
CHAPTER 3: 2-D BEAMFORMING CODE OPTIMIZATION 12
3.1 Introduction 12
3.2 Data Acquisition 13
3.3 Geometry for computation of delays 13
3.4 Calculation of focusing delay 14
3.5 Calculation of angle of refraction 15
3.6 2-D Beamforming 16
3.7 Gaussian filter approach 18
3.8 2-D Code Optimization 19

3.9 Results 20

CHAPTER 4: IMPLEMENTATION OF 2D BEAMFORMING ON DSP KIT 21

4.1 Introduction 21

4.2 Comparison of DSP kits 22

4.3 TMS320C6713 Digital Signal Processor 23

4.4 Functional Overview of DSP Board 24

4.5 Software 26

4.6 Components of CCS 27

i. Code Composer Studio Setup: 27

ii. TMS320C6713 DSK Diagnostic utility: 27

iii. Code Composer Studio Integrated Development Environment (IDE): 28

iv. DSP/BIOS plug-ins: 30

v. RTDX plug-in: 30

4.7 2D Beamforming Algorithm 31

i. C Language Programming: 31

ii. RTDX link between CCS and MATLAB: 32

iii. Memory Management: 34

Chapter 5: 3D BEAMFORMING 36

5.1 Introduction 36

5.2 Data Acquisition for 3D beamforming 36

5.3 Approach using transformation matrix 37

5.4 Computation of delays 38

5.5 Dimensional Beamforming 39

5.6 Calculation of angles 40

5.7 Rotation matrix 41

5.8 Results: 43

5.9 Approach using permittivity analysis 44

5.10 Geometry of the scene 44

5.11 Assumptions regarding permittivity of wall 45

5.12 Calculation of points of refraction 46

5.13 Calculation of propagation delay 47

5.14 Results 47

5.15 Comparison 48

5.16 Cubism 49

CHAPTER 6: FUTURE WORK 51

REFERENCES 53

ANNEX A: OPERATING MANUAL 55

LIST OF TABLES

2.1 Antenna Specification. 7

4.1 Comparison of DSP kits. 22

LIST OF FIGURES

"Images in this thesis are presented in color"

2-1 Project overview. 5

2-2 Antenna Design. 7

2-3 VNA back View 9

2-4 PIC 16f84 Pin Configuration. 11

3-1 Geometry for computation of travelling distances 15

3-2 Pixels in room to be scanned 17

3-3 Data Allignment in form of a cube 19

3-4 Previos image and image after applying cubism.. 20

4-1 TMS320C6713 DSP Kit. 23

4-2 Functional Block Diagram of TMS320C6713 DSP kit. 24

4-3 Program Development flow in CCS 26

4-4 CCS Setup Utility. 27

4-5 DSP Diagnostic utility 28

4-6 CCS IDE. 29

4-7 Composite Block Diagram of DSP system 31

4-8 Memory Map of C6713 34

4-9 Memory Management 35

5-1 Geometry for 3D imaging. 37

5-2 2-Dimensional Hamming Window. 39

5-3 Angle β between (x_q,y_q) and (x_{tm},y_{tm}). 42

5-4 The transformation of (x,y) plane. 43

5-5 Image of Human sitting beyond the wall 44

5-6 3D Scene of target area 45

5-7 Image of Human Standing beyond the wall 47

5-8 Image of a parabolic reflector placed beyond the wall. 48

5-9 Cube encapsulating 3D matrix in 3D beamforming 50

LIST OF SYMBOLS/ ABBREVIATIONS

TWMI	Through the wall microwave imaging
2D	Two Dimensional
3D	Three Dimensional
UWB	Ultra wideband
E or *H*-plane	Electrical or Magnetic plane
VNA	Vector network analyzer
HFSS	High frequency structure simulator
RF	Radio Frequency
dB	Decibels
R	Taper rate
S11	Reflection parameter from port 1 to port 1
A	Width of waveguide
B	Length of waveguide
D	Height of waveguide
L	Axial length
L + d	Total length
W	Width of ridges

H	Height of ridges
R	Radius of circular ridge in waveguide
S21	Reflection parameter from port 2 to port 1
LAN	Local Area Network
UTP	unshielded twisted pair
RJ-45	Connector used for LAN port
FTP	File Transfer Protocol
DC	Direct Current
PIC 16F84	Microcontroller model number
IR	Infrared
RS-232	Serial port
GUI	Graphic user interface
RAM	Radar absorbent Material
SAR	Synthetic Aperture Radar
C or V	speed of lights in air and wall respectively
θ_{wall}	Angle along the wall
θ_{air}	Angle in air
ε_{wall}	permittivity of wall

$l_{mp,air,1}$	length covered by wave in air before striking wall
$l_{mp,wall}$	length covered by wave while passing
$l_{mp,air,2}$	length covered by wave in air between the wall and the target pixel
x_q, y_q, z_q	pixel coordinate points along x-axis, y-axis and z-axis
τ_{mp}	Focusing delay
h(t)	impulse response of matched filter
T*	denoted the complex conjugate for T
g(t)	Gaussian pulse symbol
$g^2(t)$	Gaussian filter second derivative
α	pulse shaping factor
$E_q(t)$	weighting factor
DSK	Digital Signal Processing starter kit

CHAPTER 1: OVERVIEW

1.1 Introduction

Microwave Imaging is a technique used in sensing a given scene by means of interrogating microwaves, it is generally perceived as the reconstruction of permittivity distribution function of the medium under consideration from the measurement of the scattered electromagnetic fields interacting with the medium. It has recently proven its usefulness in providing excellent diagnostic capabilities in several areas, including civil and industrial engineering, nondestructive testing and evaluation, geophysical prospecting, and biomedical engineering. Through the wall imaging is one of the fields of microwave imaging in which a lot of interest has been seen recently, it consists of a setup in which a target is to be localized and reconstructed by using an imaging system positioned behind a wall or another blinding structure. The main purpose is for security but other surveillance applications are also possible. Radar techniques have been proposed mainly for this purpose but other approaches, like inverse scattering based imaging can also be adopted.

One of the most crucial parts of the microwave imaging process is the development of an efficient algorithm for reconstructing the depth dependent profiles of objects from the measurement of scattering coefficients. Along with an optimized 2D and 3D code an innovative experimental setup is also described here for the free-space and through the wall microwave imaging of objects.

Assuming the target or volume illuminated is composed of point-like scatterers, the received signal consists of a sum of scaled and delayed versions of the transmitted signal.

The received signals give range information about the location of targets, but no azimuth information other than that deduced from knowledge of the antenna beam width and volume of illumination. However, when antenna is moved in multiple vertical and horizontal planes, it is possible to determine azimuth information about a target as well.

The principal goal of this project is to compose an effective image processing algorithm to accomplish effective imaging of various objects through walls using microwave frequencies.

1.2 Problem statement

Imaging through wall was initiated in Pakistan by the students of MCS last year[2], keeping in view the considerable work done by them and being the need of the hour due to the environment prevailing in the country we decided to pursue it and enhance it to the next level i.e. to optimize 2D coding by decreasing the processing time as well as development of a 3D code.

1.3 Scope/ objectives

The project has the following objectives:

i. To optimize the existing algorithm [2] for 2D beamforming
ii. Implementation of digital signal processing on a dedicated processor
iii. Up gradation of existing hardware to suite 3D image scanning
iv. To develop 3D imaging capability for intuitive image interpretation
v. Development of the 3D algorithm
vi. Testing using various data sets

1.4 Applications

The through the wall imaging technologies can detect the radiation reflected from an object when illuminated with microwaves, utilizing the capability of microwaves to penetrate through opaque materials. This radiation can provide sufficient information about the object, providing the image of its external surface. There are a number of applications of microwave imaging through the wall technology including security, medicine and defense etc.

i. Healthcare: Microwave imaging uses less-intrusive imaging techniques, meaning that the equipment used is less physically intrusive upon a patient and using safer doses of radiation. These techniques could be used instead of traditional X-rays which have extensive levels of radiation so have a limited usage per person. Microwave imaging techniques could be used to diagnose breast cancer or tumors in human body at early stage.

ii. Security: The surveillance of people cannot make use of ionizing and intensive radiation for safety purposes [16]. The current metal detection solution is limited as it cannot see underneath clothing. The microwave imaging provides an obvious advantage in being more reliable, covert, and less disruptive to passengers at airports, railways, or to people entering buildings through security checkpoints.

iii. Defense force: In the modern battlefield environment, the necessity to counter asymmetric threats has resulted in a significantly increased possibility that military ground forces will need to handle and neutralize hostile situation in an urban environment, where the enemy may be hidden in one of a number of buildings. In this scenario, the warrior's situational understanding is often severely reduced, which may result in heightened personal danger and increased risk of collateral damage. Therefore, many defense agencies have shown keen interest in developing the Sensing through the Wall (STTW) technologies. The need is to develop a device that is portable enough to be used anywhere to acquire scanning data and which can support fast real time processing to construct the effective image of the scene behind the walls.

CHAPTER 2: BACKGROUND

2.1 Introduction

In 2010 a group of students at Military College of Signals initiated work on through the wall imaging using microwaves; being the pioneers of this field in Pakistan they did a tremendous amount of work [2]. Although the reference work only catered for the 2D imaging, that took a lot of computational time. However it was a mile stone in this field, their work consisted of four modules: antenna designing, construction of a positioner, an anechoic chamber and development of algorithm for 2D beamforming. These modules are shown in Figure 2-1.

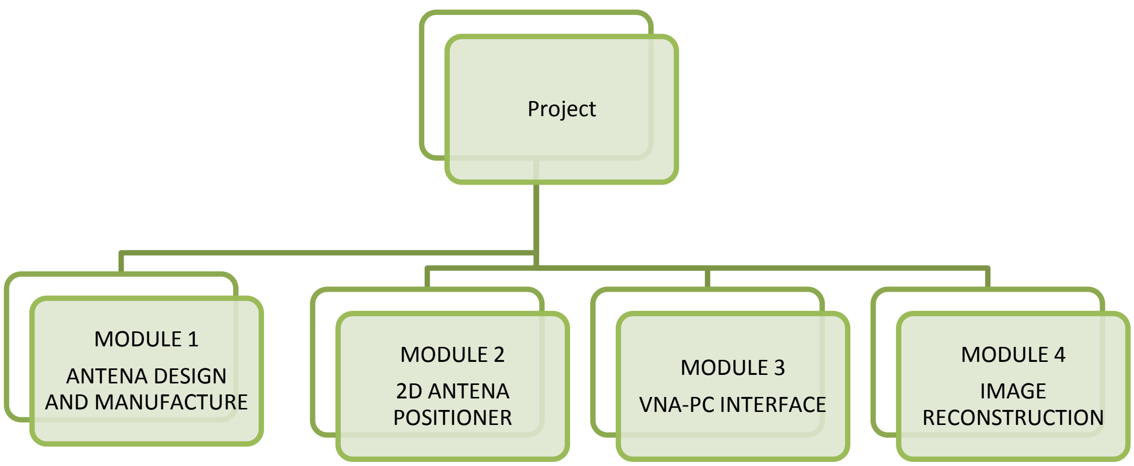

Figure 2-1: Project overview

The beamforming algorithms are generated in MATLAB and Code Composer Studio. The hardware setup consisted of a horn antenna mounted on a positioner in a synthetic aperture radar architecture that is interfaced with a computer system running MATLAB through the VNA.

2.2 Antenna specifications

From the Radar signal processing point of view, to design any imaging system with satisfactory performance, such as ability to detect and distinguish moving and stationary objects, their dimensions, speed and locations, an antenna must satisfy some of the requirements including; optimum performance for the desired frequency range, it should not have large electrical size either to be spatially big or to have a wide bandwidth, or, even better, to possess both features. These features are responsible for spatial, or range, resolution, both azimuth and elevation, It should have a reasonable gain, It should have a directional radiation pattern so that most of the radiated power is concentrated in a narrow beam and we do not get unwanted reflections for other objects, It should be physically small, low-profile and low-cost. All these features are important to create low-cost, convenient TWMI system, it should be easy to mount, easy to match, have good transmission and radiation performance.

Before designing an antenna for TWMI, there is a need to select appropriate frequency range. The signal should have enough penetration through wall and resolution is required to get precise location of the objects present behind the wall. It is known that at lower frequencies we get more penetration but at the same less resolution. Similarly at higher frequencies we can have more resolution (due to smaller wavelengths) but less penetration. So a trade off is required. Therefore, S-band (2-4GHz) can be used for antenna operation in order to get optimum results. Moreover the vector network analyzer (VNA) available, for signal generation and reception, has the frequency range from 300 KHz to 3GHz. Hence workable frequency range is from 2GHz to 3GHz with 1nsec resolution. An antenna for frequency range 2 to 4GHz was required. High frequency structure simulator (HFSSv11) was used to design the antenna as shown in Figure 2-2, as it has been observed that its simulated results closely resemble manufactured results.

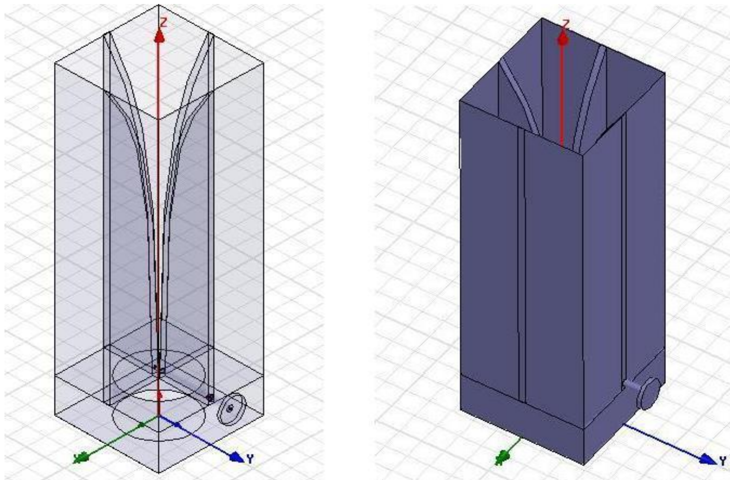

Figure 2-2: Antenna Design

A square quad-ridged horn antenna was fabricated to have more directional pattern. Table 2-1 gives the design parameters of the simulated antenna. The measured results were highly satisfactory revealing large impedance bandwidth with criteria (S11 < -8dB) at the range of frequencies (1.5 t0 4GHz) used for through the wall microwave imaging. Also, good antenna performances such as radiation patterns and antenna gains over the operating bands were observed. Also the gain of the simulated model was found out to be approximately 13 dB.

Table 2-1: Antenna dimensions

Design parameters	Symbols	Values (cm)
Width of waveguide	A	11.04
Length of waveguide	B	11.04
Height of waveguide	D	3.84
Axial length	L	29.76

Total length	L + d	33.6
Width of ridges	W	0.6
Height of ridges	H	4.92
Taper rate	R	0.15
Radius of circular ridge in waveguide	R	3.48

2.3 VNA-LAN interface

Vector Network Analyzer (VNA) is used as microwave signal generator and recording reflections. Agilent's 8714ET analyzer with a frequency range 30 KHz to 3 GHz is used to generate microwave signals in 2-3 GHz range at 201 points. It can measure scattering parameters for reflection and transmission S11 and S21 respectively. These are transmitted through horn antenna and scattering parameter S11 is measured over VNA screen as smith chart. To transfer this data to Processing workstation (PC); LAN port was used.

2.4 Connecting/configuring the analyzer to LAN

A single computer was connected with a single analyzer, avoiding a LAN hub. To do this, a special "cross-over" cable or adapter was used, which acts like a LAN hub, as a point-to-point connection using a standard "straight-through" cable, does not work. For most applications, the use of a LAN hub is simpler, and additional devices can be added easily. To connect the analyzer to your network the following steps of Turning off the analyzer, connecting the Ether-twist cable from your network to the LAN Ether-twist port on the rear of your analyzer and turning on the analyzer are carried out. Figure 2-3 [18] shows the back view of the VNA showing different ports available for interfacing.

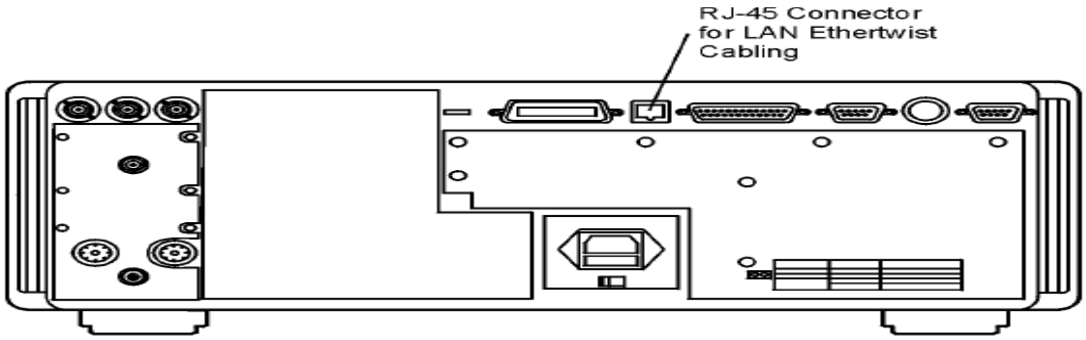

Figure 2-3: VNA-back view

2.5 LAN-FTP interface

Network Analyzer has an ftp directory called "data," which is a dynamic data disk. The files in this directory trigger analyzer operations. For example, an instrument state into this directory and the analyzer will automatically recall this state. Copy this to the analyzer's data directory and it will automatically run. Transferring of a screen-image file from the analyzer in GIF, PCX, or HP-GL formats also possible.

MATLAB and Code Composer Studio (CCS v3.1) are used as processing software in this project, so all the required data in analyzer's memory is to be accessed to it for further analysis and radar signal processing.

2.6 2D Antenna Positioning Assembly

A positioning mechanism, on which the antenna can be mounted and moved in an accurate and controlled fashion, was constructed for imaging process to commence. The Positioner was designed keeping in view the requirements of the imaging process. It has to have a good precision since the precision of the imaging process depends on it. Furthermore, it has to be controllable and interface-able with computer to automate the positioning process and to accommodate for control of Positioner from within the algorithm in the final integrated system. The Positioner design finalized was decided to have a scan area of 6’ by 8’. This allowance was made to keep provision of usage of this Positioner in future for other experiments/applications as well. This frame is mounted on the 3’ by 3’ stand. Its main purpose is to provide stability to the Positioner frame as well as to keep it above ground to minimize ground reflections. For movement of the antenna assembly (in both dimensions), chains (typically used in motorcycles; easily available) along with sprockets are used. A slight imprecision is introduced due to ‘play’ while using these chains. The chains are fixed to the frame while sprockets are attached to motors on the assembly.

A DC motor was selected, which is a motor commonly used in car windshield wipers. It was found to have very small backlash and generated enough torque to manage the application properly. Initially it was thought to use some proper breaking mechanism for motors, however, due to the slow speed of operation and small backlash of motors, it was not considered being required anymore. DC wiper motor being a high torque motor has high power requirements. It drew more current (typically around 2-3A). Microcontrollers provide currents usually of the order of 50mA. So an intermediate driver stage had to be made externally to drive and control these motors. H bridges using relays with considerable current ratings were used for the driver stage. Motion in both dimensions is achieved using two separate motors both of which, based on the need, had to be moved in both directions. This requirement is met using 4x5pin relays in an arrangement shown in the Figure 2-4 [19]. To enable relays to be effectively switched on from the controller pulses, Darlington pairs are used to amplify current. The Opto-couplers are also used for effective switching, isolating the H bridge from the controller. The microcontrollers used were PIC 16F84 and PIC 16F872 due to their efficient working, easy of availability, convenience in using its compiler Micro Code Studio.

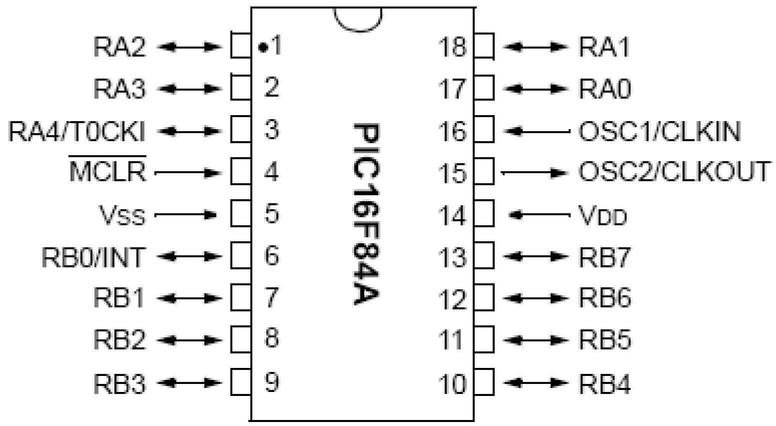

Figure 2-4: PIC 16f84 pin configuration

Position based control was used to control Positioner movement. Encoders are employed for this purpose. These encoders consist of an IR transmitter, Receiver and a disk with a number of slits. These disks are mounted on the motor shafts and when they move with the motors these slits cut the IR beam generating pulses. These pulses are counted by the microcontroller and give an accurate estimate of distance covered by the motor. By dividing the distance covered by sprocket in one rotation(it's circumference) by the number of pulses given in one rotation (equal to number of slits in the disk), one can easily calculate the number of pulses corresponding to any step size being input from the user. Then, by turning the motor on and off based on that count an accurate distance and position control is maintained.

CHAPTER 3: 2-D BEAMFORMING CODE OPTIMIZATION

3.1 Introduction

For SAR beamforming, the algorithm is applied to experimental data that is obtained for various radar scene configurations that includes placing different objects in free-space or placing beyond the wall. Data are collected with the wideband Radar Microwave Imaging System, which uses a single Quad Ridge Horn antenna that acts as a transceiver and operating in the frequency range from 2 to 3 GHz. This antenna mechanically scans the entire room by acquiring readings at discrete locations, in this way this mechanism avoids the common coupling that occurs in the case when an array of antennas is used. Measurements are performed in the frequency domain at several discrete frequencies with the help of VNA. VNA is also providing excitation to the antenna in the required frequency range so that optimum resolution and penetration capability in through the wall scenario is obtained. Scattering parameter S11 is measured by VNA in terms of Phase and magnitude information and recorded in computer system corresponding to each step of antenna position. Once the 2D data is captured, it is further processed using MATLAB first for extracting useful information from the received files from VNA. The algorithm processes the received signals in a medium whose permittivity is known, this medium may either be free-space or a wall with known permittivity, to achieve effective imaging. The results obtained using both of the configurations models are investigated, processed and compared.

3.2 Data Acquisition

For TWMI, a step-frequency radar (SFR) approach [3] is applied for generating a broadband pulse. Continuous wave measurements of both magnitude and phase at several closely spaced discrete frequencies are collected over a broad frequency band of 2-3 GHz. For the Step Frequency Radar approach, the measurement system can be easily built around a microwave vector network analyzer with relatively less additional components. However, data collection time is increased in general because the antenna makes mechanical horizontal movements for a complete 2-D scan of the room. Our Radar uses the 1GHz band with step size of 5 MHz; data is collected at discrete positions at 201 frequencies between 2 and 3 GHz. It makes a sampling time of 1ns in time domain and 30 meters Radar range. Similar 2D data is acquired at different antenna locations and stored in form of matrices with the aid of VNA and MATLAB. The stored data is actually S11 parameter with the information of phase and magnitude of the reflected signal from the target beyond the wall.

3.3 Geometry for computation of delays

The geometry of data acquisition scenario for scanning a 2-D scene is now explained. Let the wall through which imaging is to be performed is be of uniform thickness d, and of some known permittivity ε, the wall lies in *(x,y)- plane* and the horizontal line on which antenna is moving is parallel to x-axis in the *(x,z) plane*. The antenna is placed at a distance z_{off} from the wall. The region to be scanned is assumed to be along positive *z axis*. Let the antenna be located at m_{th} location, then its coordinates will be $(x_{tm},, z_{off})$. The antenna is illuminating the scene with a wideband signal $s(t)$. The reflections from any target are recorded from the same antenna location from which signal was transmitted. So the antenna actually acts as a transceiver. For a single point target located at $x_p = (x_p, z_p)$ the reflected signal $r_m(t)$ at m_{th} location is given by equation 3.1[1]:

$$r_m(t) = a(x_p)s(t - \tau_{mp}) \tag{3.1}$$

3.4 Calculation of focusing delay

As the signal travels from the m_{th} transceiver to the target located at x_p, it encounters some propagation delay that is given by τ_{mp}, given in equation 3.2 [1]. This is calculated by simple distance divided by velocity formula:

$$\tau_{mp} = \frac{2l_{mp,air,1}}{c} + \frac{2l_{mp,wall}}{v} + \frac{2l_{mp,air,2}}{c} \tag{3.2}$$

Where v is given by:

$$v = \frac{c}{\sqrt{\varepsilon}} \tag{3.3}$$

In equations 3.2 and 3.3 [1]:

c: Speed of light or speed of microwave as it travels through free space

v: speed of propagation while traversing through wall

$l_{mp,air,1}$: travelling distance of signal from m_{th} transceiver to the point where it enters the wall

$l_{mp,wall}$: travelling distance of signal when it passes through the wall

$l_{mp,air,2}$: travelling distance of signal from the point where it leaves the wall to the target at x_q

The ray diagram explaining the geometry of scene is given in figure 3-1 [1]:

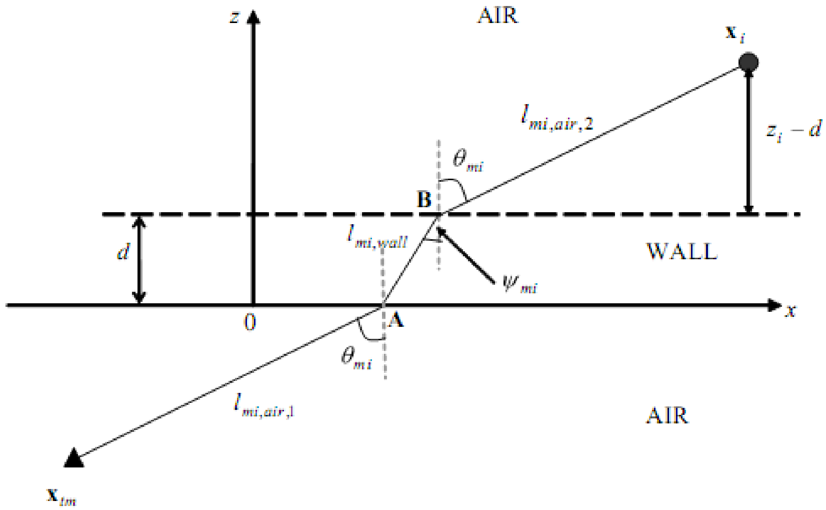

Figure 3-1: Geometry for computation of traveling distances from the m_{th} transceiver to target at x_q

This process is carried out until data is acquired from all the antenna locations. After the process of data acquisition is completed, the next step is to apply beamforming algorithm to this data.

3.5 Calculation of angle of refraction

Angle of refraction can be found if the wall thickness and dielectric permittivity is known, by applying Snell's law, angle of refraction is given by equation 3.4 as in [3]:

$$\theta_{wall} = \frac{sin^{-1}(\,Sin\theta_{air})}{\sqrt{\varepsilon_{wall}}} \tag{3.4}$$

The distances $l_{mp,air,1}$, $l_{mp,wall1}$ and $l_{mp,air,2}$ can be found by equations 3.5, 3.6 and 3.7 in [3]:

$$l_{mp,air,1} = \frac{z_{off}}{\cos\theta_{air}} \tag{3.5}$$

$$l_{mp,wall} = \frac{d}{\cos\theta_{wall}} \tag{3.6}$$

$$l_{mp,air,2} = \frac{z_q - d}{\cos\theta_{air}} \tag{3.7}$$

The above equations are in terms of angle of incidence, next we need to calculate θ_{mq}. This is calculated by considering the triangles ABx_q and applying Cosine law to derive the transcendental equation 3.8 [1].

$$(x_q - (x_{tm} + z_{off} \tan\theta_{air}))^2 + {z_q}^2 = {l_{mp,wall}}^2 + {l_{mp,air,2}}^2 - 2 l_{mp,wall} L_{mp,air,2} \cos(\pi + \theta_{wall} - \theta_{mq}) \quad (3.8)$$

The equation can be solved using numerical method to find out the unknown quantities.

3.6 2-D Beamforming

In order to perform an effective beamforming a calibration procedure is carried out, in which two measurement scenarios are incorporated. One of these scenarios is taking a scan of the entire target area while placing it beyond the wall and the other scenario comprises of taking a complete scan of the entire empty scan area, this scan is referred to as free space measurements. This process helps to remove many sources of pulse distortion in the time-domain data which occur due to the effective aperture, phase dispersion, and resonances of the antennas. Also the reflection from ceiling and floor are removed through this calibration. In addition anechoic chamber is used to absorb redundant or unnecessary signals. Further Processing is performed over the calibrated data to obtain the image of the target.

The region of interest as shown in figure 3-2 is assumed to be the *(x,z)plane*, and it is divided into finite number of pixels. Number of pixels in cross-range and down-range i.e. depth are 69 and 201 and respectively.

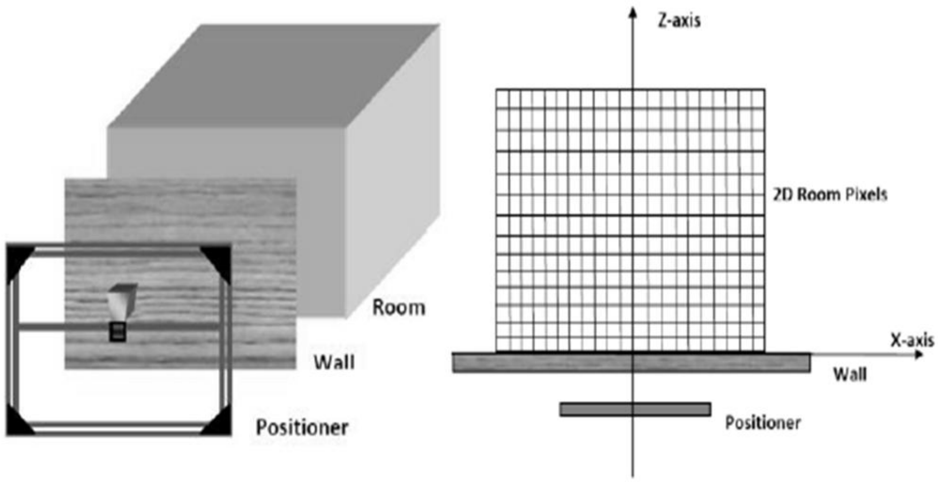

Figure 3-2: Pixels in room to be scanned

The intensity of complex composite signal that is reflected back from the target placed behind the wall can be determined by adding the value of focusing delay to the signal. This is initially done for one pixel and then for one particular antenna location, the value of intensity is calculated and summed for all the pixels as given in equation 3.9 [1].

$$y(t) = \sum_{m=1}^{M} r\left(x_{xtm}, \tau_{mp}\right) \tag{3.9}$$

Where r is the received signal, τ_{mp} is the focusing delay and m is the antenna location.

In order to improve the values of intensity, appropriate weights are applied, as given in the equation 3.10 [1]:

$$y(t) = \sum_{m=1}^{M} w_m r\left(x_{tm}, \tau_{mp}\right) \tag{3.10}$$

The weight, w_m is independent of the pixel location defined by x_q. It actually serves to control the shape and side lobe structure of the beam. The weight applied in this way is referred to as inverse distance weight because the pixel with minimum distance to antenna at certain position will get the maximum weight. The described process of applying weights is performed for all the pixels and the values of intensity for all the pixels are obtained, these pixels are then combined to construct a 2Dbeamformed image of the target. This image may also contain some of the false targets [6] which can be removed by passing the signal through a filter that is matched to the transmitted pulse *s(t)* and sampling the output signal as given in equation 3.11 [1]:

$$I(x_q) = \big(y(t) * h(t)\big)\,|_{t=0} \tag{3.11}$$

Where *h (t) = s*(t)* i.e. the complex conjugate of the impulse response of the matched filter. This process is again repeated for all the pixels in the scan area and a composite image is constructed.

3.7 Gaussian filter approach

In our algorithm, the vectors of the beamformed data are cross-correlated with the second derivative of Gaussian mono pulse. This is because the second derivative has very close resemblance to the shape of target echoes than any other derivative [4,12].

Gaussian pulse and its second derivative are represented as given in equation 3.12 and 3.13 [4]:

$$g(t) = -\frac{\sqrt{2}}{\alpha} e^{-(2\pi t^2/\alpha^2)} \tag{3.12}$$

$$g^2(t) = \left(1 - 4\pi\frac{t^2}{\alpha^2}\right) e^{-\left(2\pi t^2/\alpha^2\right)} \tag{3.13}$$

Where α is called the pulse shaping factor, value of α is 9e-10 in order to cater for the optimum shape. The cross correlation of beamformed data vectors and the second derivative of Gaussian mono-pulse signals are represented as given in equation 3.14 [4]:

$$T_q(\tau) = \int_{-\infty}^{\infty} B_q(t) g^2(t-\tau)\, d\tau \tag{3.14}$$

Now in order to improve the visibility of the target in the image obtained, the signal $T_q(\tau)$

is passed through an impulsive filter of 1 nano second interval, this is termed as envelop detection.

$$E_q(t) = (T_q(\tau))^2 * h(t) \tag{3.15}$$

The final step is to use $E_q(t)$ as the weighting factor for the beamformed image. It helps to eliminate the false targets appearing in image and to separate out the closely spaced targets in case of multiple target scenarios.

3.8 2-D Code Optimization

In order to optimize this algorithm, the concept of Cubism is implemented, in which the entire data set in encapsulated in the form of a cube such that every possible value of x_q, z_q and x_{tm} is catered for manipulation simultaneously. Figure 3-3 describes the concept of encapsulating the whole data in one cube.

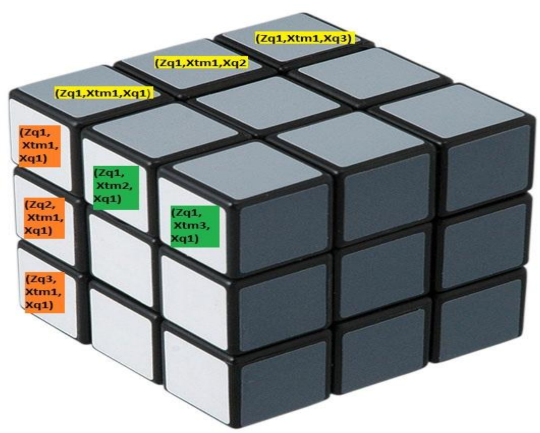

Figure 3-3: Data alignment in form of cube

Where x_{tm} are the horizontal antenna locations, x_q are the pixels in horizontal plane i.e. range and z_q are the pixels in depth i.e. downrange.

This method is first applied for the calculation of angles. This algorithm also used in solving the transcendental equations given in 3.8, to find out the angles, but since cubism facilitates the computation on a 3D matrix as a whole, the execution time is reduced to 4 minutes. Same is the case for beamforming, i.e. same equations are used but instead of applying these equations one by one on each pixel of the entire scan area, these are applied on the whole cube of comprising of every possible value in the scanning area. This process takes only 6 seconds while execution. So the total time for generating a 2D image is now 4 minutes and 6 seconds.

3.9 Results

The obtained results show that the previous algorithm and our implemented algorithm show the same results but with a significant reduction in processing time. The results shown in figure 3-4 are the images of a parabolic reflector as viewed from the top of the scanned area, thus called 2D image.

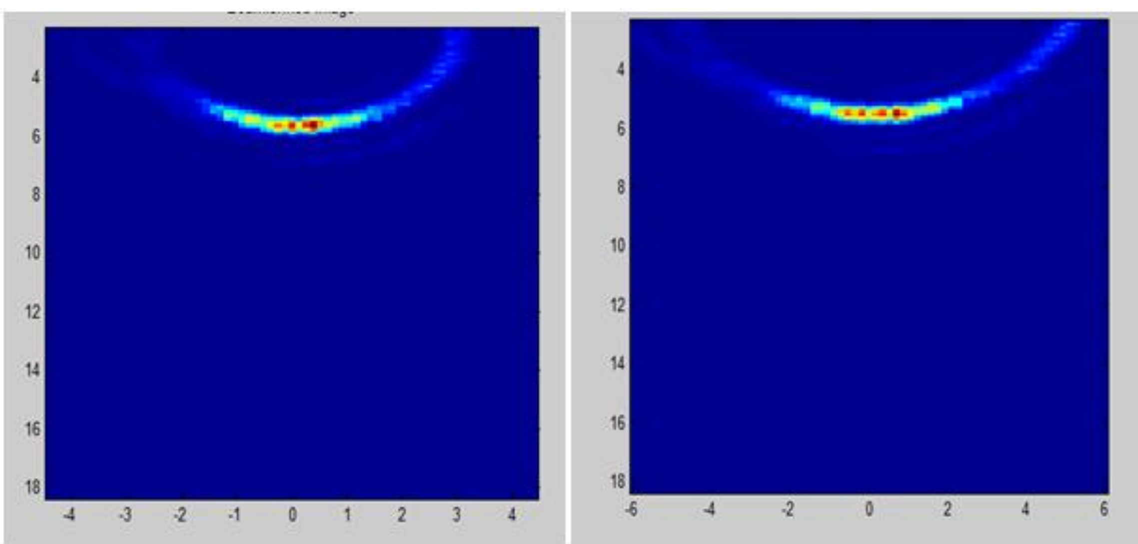

Figure 3-4: Previous image and the image after applying Cubism

CHAPTER 4: IMPLEMENTATION OF 2D BEAMFORMING ON DSP KIT

4.1 Introduction

Digital signal processors are fast special purpose processors that have specialized type of architecture. DSP comprises of an instruction set that is best suited for digital signal processing applications. The architecture of a digital signal processor is very appropriate for numerically extensive calculations. The digital signal processors can be used in a wide range of applications like in control systems, communication systems and audio and image processing. Digital signal processors can also be used for real time applications. Applications embedded digital signal processors are dominantly used in a number of products for example cellular mobile phones, fax machines and modems devices, disk drives, radio, printers, hearing aids, MP3 players, high definition television (HDTV), digital cameras, etc. These processors are preferred because they are very cost effective. They can handle different tasks, since they can be reprogrammed for a different application.

DSP techniques have been very successful because it provides the development of low-cost software as well as hardware support. For example, modems and speech recognition can be less costly using DSP techniques. For real time environment, the processor needs to be updated with some external input; this input may be analog or digital. DSP based systems are less affected by environmental conditions.

DSP processors provide the advantages of microprocessors, which are designed specifically for signal processing applications. Commonly used operations in signal processing applications are convolution, filtering, and frequency-time domain conversions. These operations need iterative multiplications and additions referred to as multiply and accumulate (MAC) operations. Standard microprocessors take a lot of time for performing MAC operations. However, DSPs contain specialized units that can execute the same MAC operation in a single machine cycle.

4.2 Comparison of DSP kits

Digital Signal Processing Kit (DSK) that we are using is manufactured by Texas Instruments. A large number of kits have been manufactured by Texas Instruments, each one having its own unique features. The processor of these kits is manufactured by Spectrum Digital Corporation. A small table of comparison of some common DSP kits available is given in table 4-1 [8]:

Table 4-1: Comparison of different DSP kits available

TMS320C6416	*TMS320C6713*	TMS320VC5510	*TMS320VC5416*
Operates at 1 GHz	Operates at 225 MHz	Operates at 200 MHz	Operates at 16-160 MHz
Fixed point processor	Both Floating and fixed point processor	Fixed point processor	Fixed point processor
2M x 64 on board SDRAM	2M x 32 on board SDRAM	8 MB on board SDRAM	64K words of on board RAM
512K bytes of on board Flash ROM	512K bytes of on board Flash ROM	256K words of on board Flash ROM	256K words of on board Flash ROM

The features the kits have in common are:

i. Embedded USB JTAG (Joint Test Action Group) controller with plug and play and play functionality provided with USB cable

ii. 3 Expansion connectors that can be used for Memory Interface, Peripheral Interface, and Host Port Interface

iii. On board IEEE 1149.1 JTAG connection for optional emulator debug

iv. 4 user definable LEDs

v. 4 position dip switch, user definable

vi. +5 Volt operation only, power supply

According to the processing and memory requirements of our algorithm, TMS320C6713 is the appropriate kit, as it is a floating point processor that operates at 225 MHz, in addition 2Mx32 SDRAM fulfills our memory requirements.

4.3 TMS320C6713 Digital Signal Processor

The TMS320C6713 or commonly known as C6713, in figure 4-1 [6], is a floating point processor, its architecture is VLIW based, i.e. Very Large Instruction Word, which each instruction is processed if the previous one has been processed. C6713 is well suited for numerically intensive calculations. The internal program memory is structured so that a total of eight instructions can be fetched every cycle. For example, clock rate of 225MHz, C6713 is capable of fetching eight 32-bit instructions every 1/225MHz or 4.44ns.

Figure 4-1:TMS320C6713 DSP Kit

The main features provided by TMS320C6713 are:

i. Operating frequency of 225 MHz

ii. 2M x 32 on board SDRAM

iii. 512K bytes of on board Flash ROM

iv. 3 Expansion connectors (Memory Interface, Peripheral Interface and Host Port Interface)

v. On board IEEE 1149.1 JTAG connection for optional emulator debug

vi. 4 user definable LEDs and 4 position dip switch that are user definable

vii. Power requirement of +5 Volts

viii. Size of the board 8.25" x 4.5" (210 x 115 mm), 0.062 thick

ix. Compatible with Win 98, SE, 2000, XP

4.4 Functional Overview of DSP Board

The TMS320C6713 is a very powerful signal processing chip in itself but a complete board is required that contains necessary components to take the programs and data into the chip for processing and also take data out of chip after processing is complete [6].

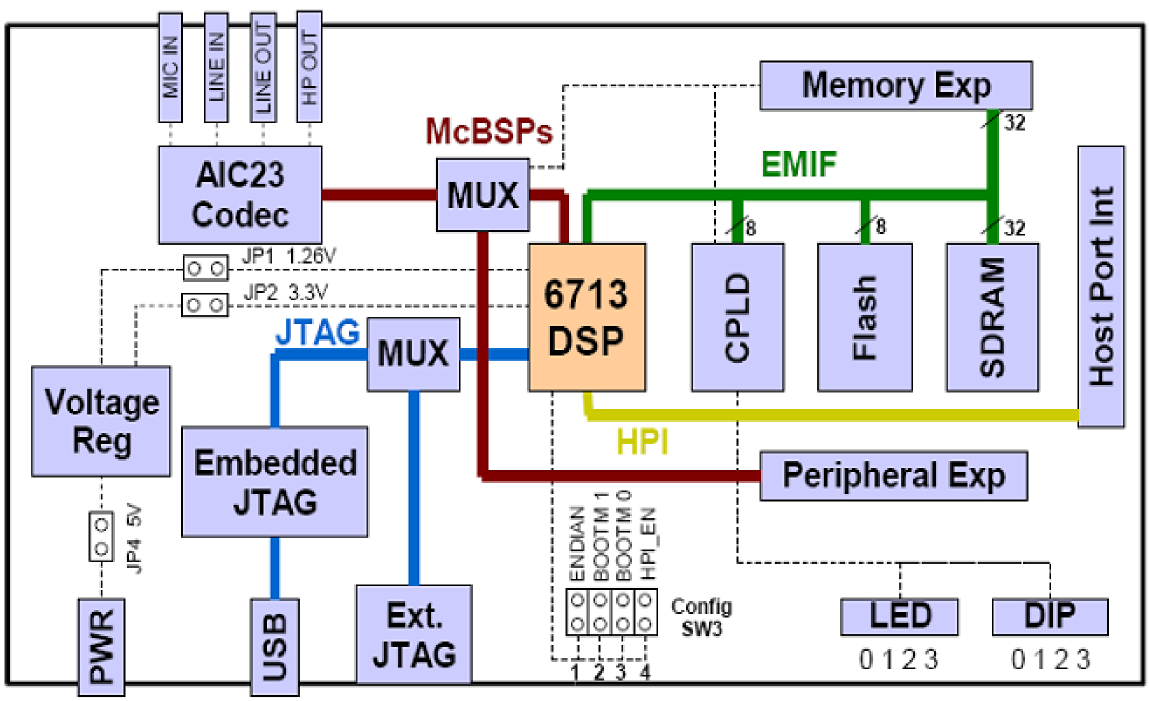

Figure 4-2: Functional Block diagram of TMS320C6713 DSP kit

Figure 4-2 [6] shows the functional block diagram of TMS320C6713 DSP kit. The major components of the DSP kit are explained briefly:

i. The DSP on the 6713 DSK can be interfaced to on-board peripherals through a 32 bit wide EMIF (External Memory Interface). EMIF signals can also be used for daughter cards, which can be used to connect any additional hardware to the DSK.

ii. The host port interface (HPI) is a parallel port through which the host processor can directly access the CPU memory space.

i. The DSP can interface to analog audio signals through an on-board AIC23 codec and four 3.5 mm audio jacks for audio input and outputs with microphone input, line input, line output and headphone output.

ii. CPLD (Complex Programmable Logic Device) is a programmable logic device that is used to implement logic that ties the board components together. The SDRAM, Flash and CPLD are all connected to the bus.

iii. The DSK includes 4 LEDs and a 4 position DIP switch which allow for interactive feedback.

iv. The JTAG connector is used to connect the board with computer. It has plug and play functionality.

v. Power input is required to be +5 volts.

vi. A 512 Kbytes on board Flash ROM is available.

vii. Expansion ports are also available to connect external devices like external memory or some display unit.

4.5 Software

The software programming tool that is used to program DSP board is Code Composer Studio (CCS v3.1) [5]. CCS is provided with the complete package of TMS320C6713 including a number of utility software tools. It is a powerful integrated development environment that provides is used to translate a high-level (C language) DSP program to an on-board machine language program. CCS is used to develop, compile and link programs that are downloaded from a computer to DSP hardware.

CCS consists of a set of software tools and libraries for developing DSP programs [5], compiling and linking them into machine code, and writing them into memory on the DSP chip and on-board external memory. It also contains diagnostic tools for analyzing and tracing algorithms as they are being implemented on-board. These components are discussed in detail below as shown in figure 4-3 [6].

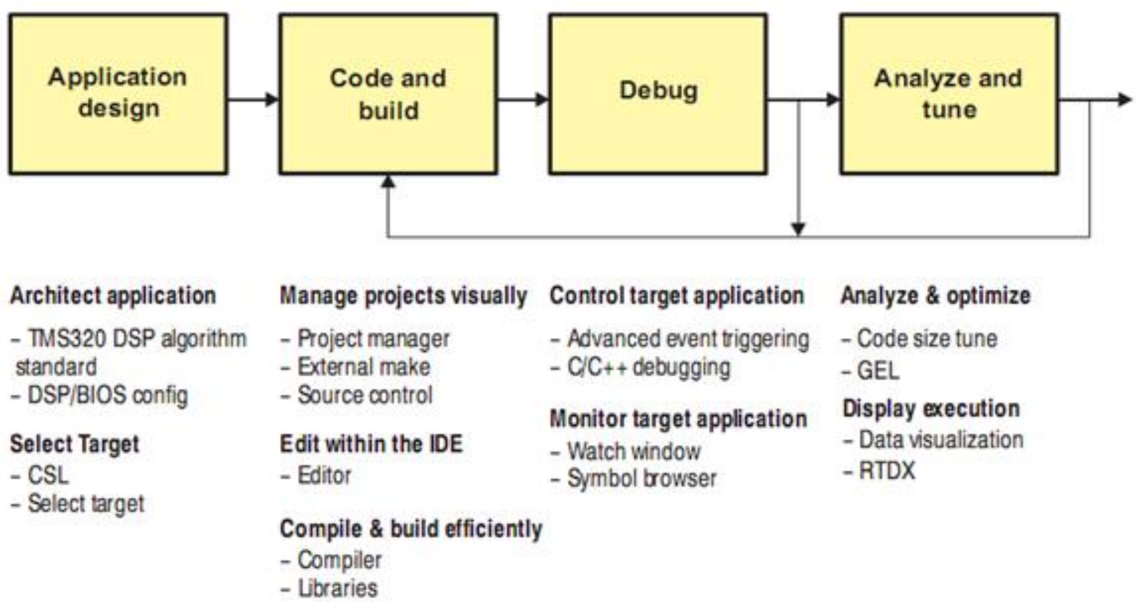

Figure 4-3: Program development flow in CCS

4.6 Components of CCS

Code Composer Studio includes the following components:

i. Code Composer Studio Setup:

The Code Composer Setup utility is used to set up the target configuration. It can be used for both single processor and multiprocessor configurations. The Setup utility, as shown in figure 4-4, helps to configure the software to work with different hardware or simulator targets.

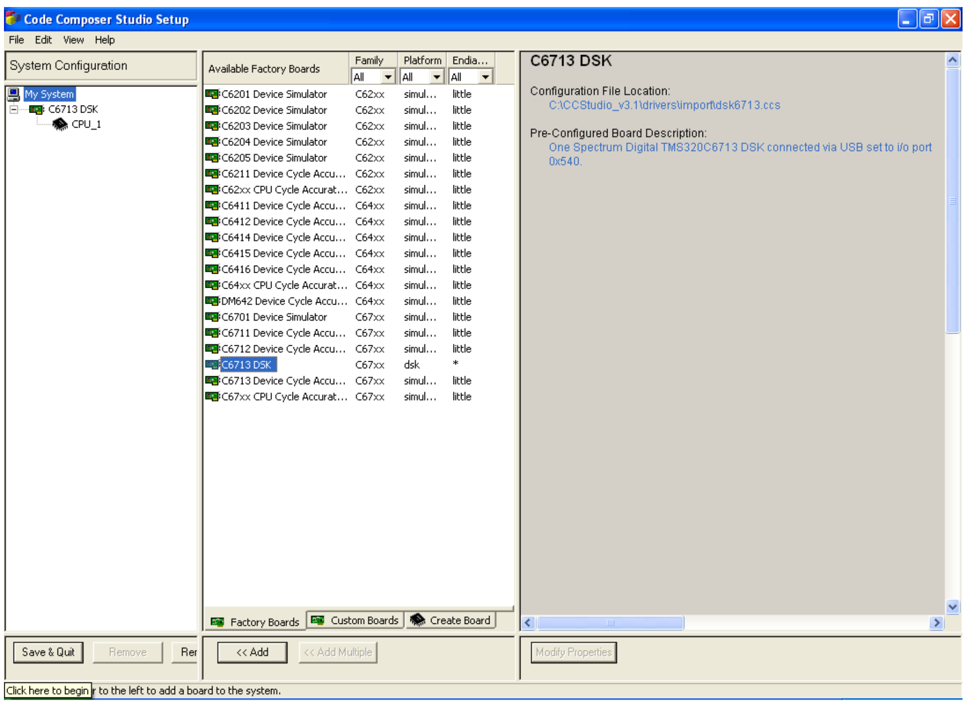

Figure 4-4: CCS setup utility

ii. TMS320C6713 DSK Diagnostic utility:

In very general terms, the diagnostic utility, in figure 4-5, helps to check if the DSP kit is going to work properly or not. The diagnostic test exercises the specific features of C6713 in order to facilitate debugging. It also lets the user to reset the DSK and emulator. It performs various checks including:

1. USB diagnostic: checking and verifying the JTAG connection with computer

2. Emulation diagnostic: verifying whether the programs developed in C will be correctly mapped to the C6713 processor
3. DSP Diagnostic: check whether C6713 processor is ready to operate or not
4. External memory diagnostic: if any external memory is being connected, this test verifies the connection
5. Flash Diagnostic: check the availability of flash memory space
6. Codec diagnostic: verifying the interface between DSP and audio codec AIC23
7. LED and DIP switch Diagnostic: verify the working for 4 LEDs and 4 user defined DIP switches

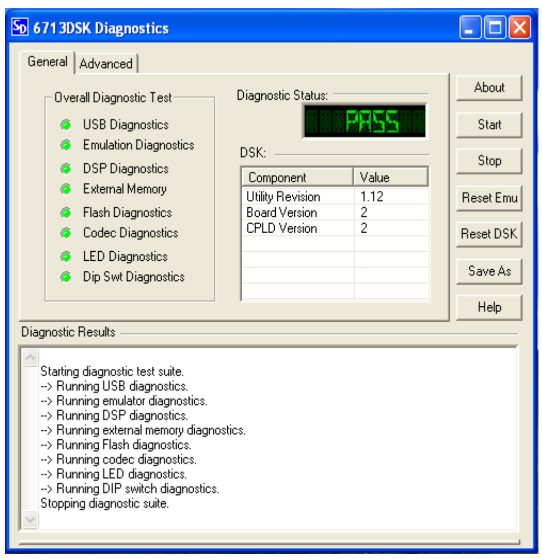

Figure 4-5: DSP Diagnostic utility

iii. Code Composer Studio Integrated Development Environment (IDE):

The Code Composer Studio Integrated Development Environment (IDE), as shown in figure 4-6, is designed to edit, build, and debug DSP target programs. This IDE incorporates a number of software tools, including tools for code generation, such as a C compiler, an assembler, and a linker. It has graphical capabilities and supports real-time debugging. It provides an easy-to-use software tool to build and debug programs. The C compiler compiles a C source program with extension *.c* to produce an assembly source file with extension.asm. The assembler assembles the *.asm* source file to produce a machine language object file with an extension *.obj*. The linker combines object files and object libraries as input to produce an executable file wit extension *.out*. This executable file can be loaded and run directly on the C6713 processor.

Besides the process of code generation, some necessary files are also needed to be added to a program to properly run on DSP; these files may be c source code, assembly source code, library files, linker command files etc. IDE facilitates this process by displaying a window that shows the complete hierarchy of files in a project. The IDE also facilitates debugging of codes by using breakpoints, watching variables etc.

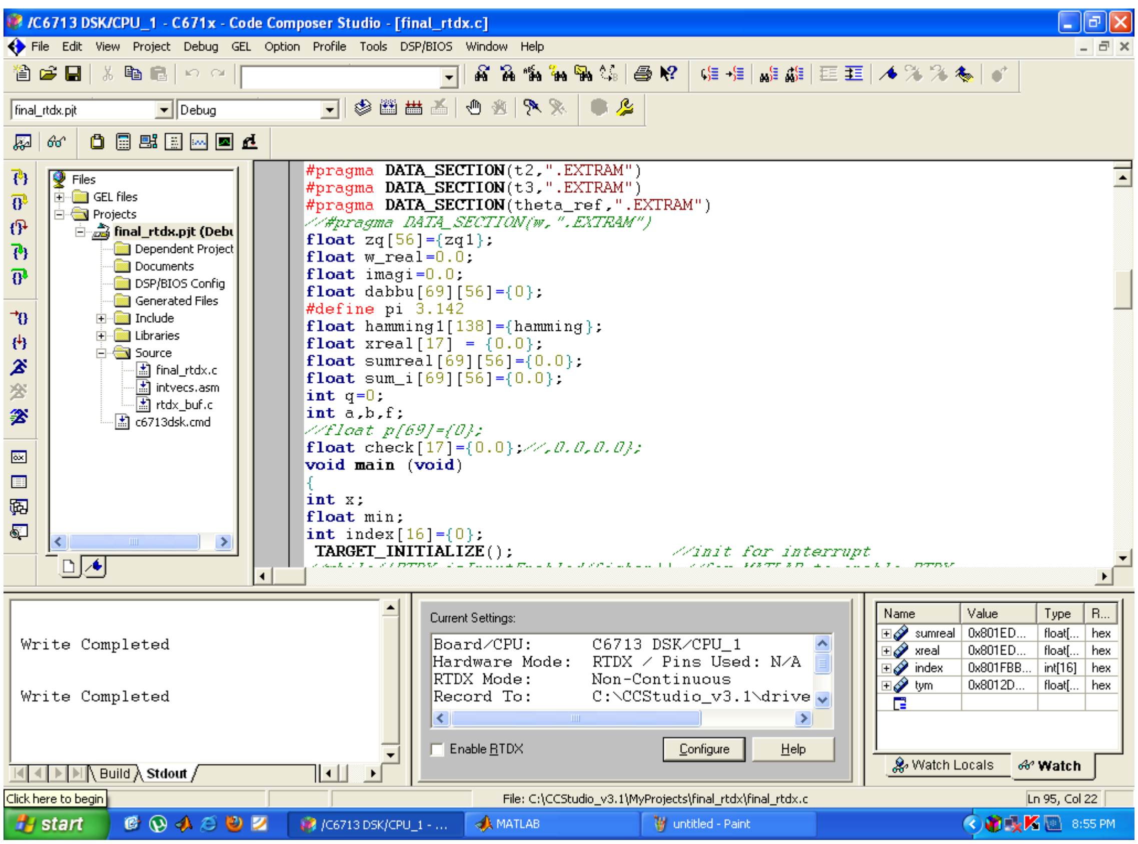

Figure 4-6: CCS IDE

iv. DSP/BIOS plug-ins:

The DSP/BIOS provides an efficient method for real-time analysis and peripheral configuration services. It eliminates the need to develop and maintain custom DSP operating systems; user can develop his system according to his requirement. A number of configurations that can be adjusted using DSP/BIOS are managing memory maps, handling interrupts and handling I/Os etc. In a particular application, the operating system and the program that has to be executed are embedded together to the DSP. DSP/BIOS handle necessary operations on the background of the running program.

v. RTDX plug-in:

Real-time data exchange (RTDX) allows the exchange of data between the host computer and the processor. RTDX consists of both target and host components. It allows data to be transferred with the aid of some other applications like MATLAB, Visual Basic, Visual C++ and LABVIEW etc. We are using MATLAB for this purpose. When RTDX data is being displayed, the host computer's applications can read it in real time and also can save data. In order to establish the RTDX link, the library file *rtdx.lib* must be included in the project. In order to pass data to or from RTDX link, the DSP application makes function calls to this library. The *rtdx.lib* uses the on-chip emulation hardware to move data to or from the host platform through the JTAG interface. Data is transferred to the host in real time while the DSP application is running [7].

These components work together as shown in Figure 4-7:

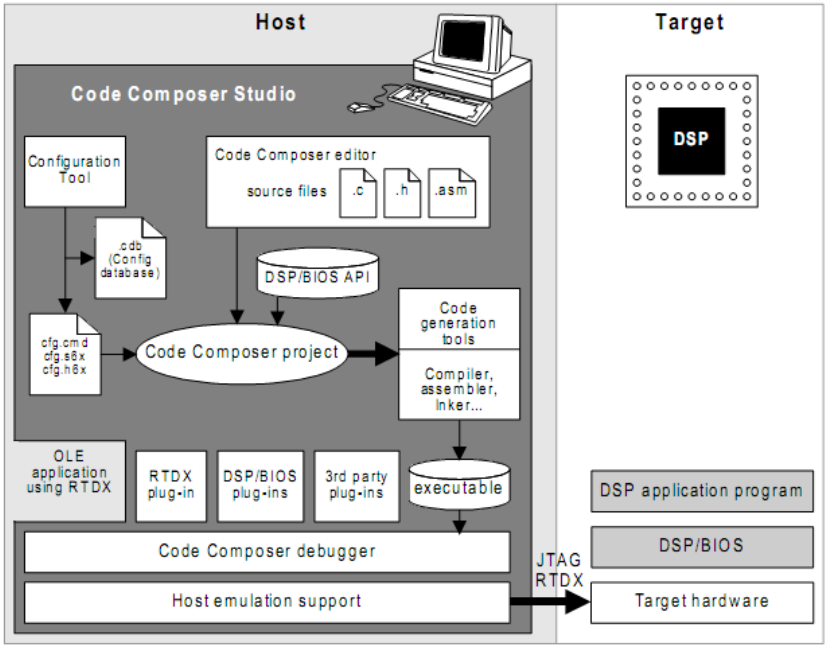

Figure 4-7: Composite block diagram of DSP system

The figure 4-7 shows that in order to develop a particular application, a new project is created in CCS, source files with extension *.c*, *.h* and *.asm* are created and included to the project. DSP/BIOS or RTDX configurations are setup according to the requirement. After including necessary library files to the project, the project is built and compiled. And eventually program is loaded onto the DSP.

4.7 2D Beamforming Algorithm

The concept implemented for 2D beamforming in CCS is same that was implemented for MATLAB coding. Same algorithm and equations are manipulated to process this algorithm on DSP. The main aspects of 2D beamforming on DSP kit are:

i. C Language Programming:

The major difference between algorithm in MATLAB and algorithm in C is the type of processing. In MATLAB, the entire data set is enclosed in form of a matrix, which is manipulated as a whole. Whereas C language processing is serial, meaning that one single value is manipulated at a time. To develop a project in CCS, its C language code is composed. Some of the support files must be added to the application, these files are discussed below:

1. *C6713dskinit.c*: this file contains functions to initialize the DSK, the codec-AIC23 and the serial ports which can also be used for I/O.
2. *C6713dskinit.h*: it is the header file which comprises of function prototypes. It consists of the features such as those used to select the microphone input in place of line input that is the default input, adjusting input gain values and so on.
3. *C6713dsk.cmd:* it is a sample linker command file. This is a generic file can be changed when a user wants to utilize the external on-board memory that is not useable in default configuration.
4. *intvecs.asm*: it is a vector file that comes with CCS and is used to handle vector operations in a code.
5. *.lib files*: a number of library files are necessary to be added, these files are *rts6700.lib*, which is run time support library for 67xx series of DSP kits. This file is contained in folder C6000\cgtools\lib. The *dsk6713bsl.lib* is Board Support Library for C6713. This file is contained in folder C6000\dsk6713\lib. The *csl6713.lib* is Chip Support Library. This file is included in c6000\bios\lib.

ii. RTDX link between CCS and MATLAB:

Real-time data exchange (RTDX) allows the exchange of data between the host computer and the processor. With RTDX, data from one application running on computer can be sent to DSP kit. As our algorithm has already been implemented in MATLAB for 2D beamforming, some of the files are stored as MAT files. These files are needed to be transferred to CCS for improving processing speed. The MAT files are actually the data that antenna is taking in form of reflections from a target behind the wall, transferring them to VNA, and then MATLAB extracts the intensity values in terms of phase and magnitude from trace file of VNA. The extracted information is stored in a MAT file and then transferred to CCS. We are not taking scanning data directly from VNA because of lack of availability of ports at DSP kit. These ports are Ethernet port that is needed to collect data from VNA and serial port that is needed to control the movement of the positioned on which antenna is mounted.

In CCS, the standard header file *rtdx.h* is included, the target DSP is initialized. After this RTDX input channel and RTDX output Channels are enabled. Once input channel is enabled, data is input to CCS, processed and after the output channel is enabled, the result of beamforming is sent to MATLAB for image construction.

In order to establish this link between MATLAB and CCS, RTDX link is established by using some commands in MATLAB. These include loading the application developed in CCS to MATLAB and making the DSP C6713 visible to MATLAB. The data rate, buffer size of the channel is also needed to be specified. RTDX channel configuration is also setup in CCS. In MATLAB, *readmsg* and *writemsg* commands are used to read and write data onto RTDX channel. Once the output is acquired in MATLAB after processing is performed in CCS, the RTDX input and output channels are disabled and closed and the running application in CCS is halted through MATLAB commands.

iii. Memory Management:

The C6713 has a two-level memory architecture as shown in figure 4-8 [20]. The Level 1 Caches are 4KB specified separately for Program and Data sections of a particular code. The Level 2 memory is 256KB, one fourth portion of this is made available as cache. The C6713 has one EMIF with four external ranges. Memory addresses are defined for each of the different section.

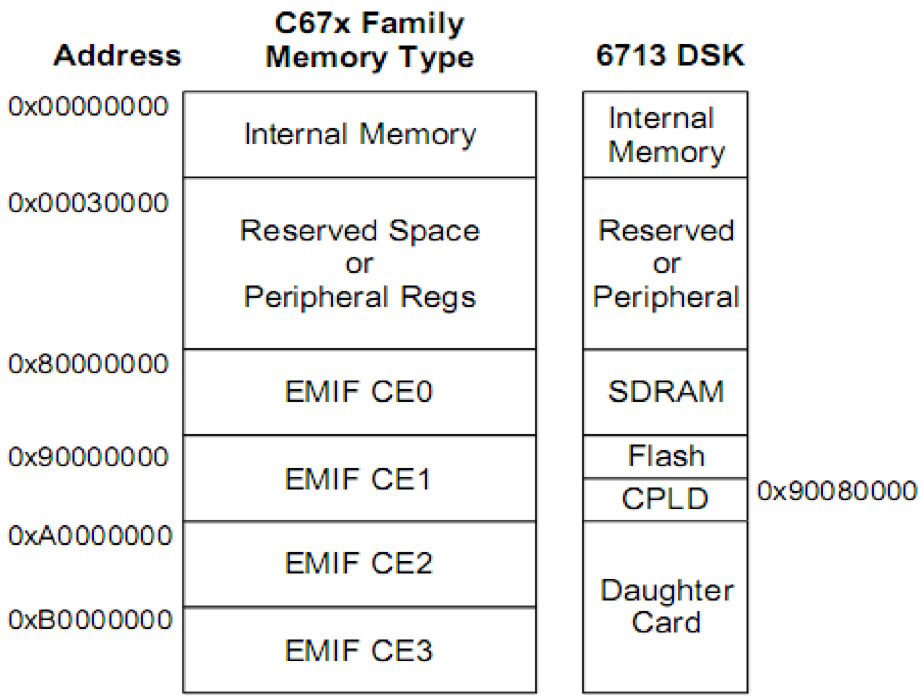

Figure 4-8: Memory Sections in C6713

Memory placement of different sections of a particular code is done according to the requirement. For this purpose a new memory section is created and the required variables that are large enough in size are mapped onto the external memory section created. This is done by executing some commands in the source file.

```
#pragma DATA_SECTION(angle, ".EXTRAM")
```

In order to introduce a new memory section, the standard header file, *mem.h* must be included to the source file. The defined memory section is also initialized in linker command file *6713dsk.cmd* so that different sections of the code are correctly mapped to their respective memory sections as shown in figure 4-9.

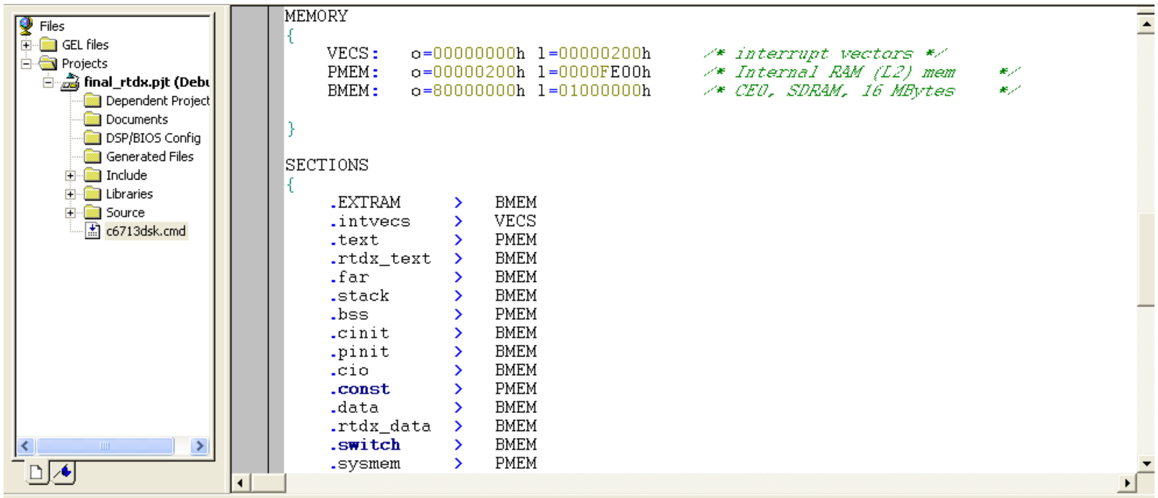

Figure 4-9: Memory Placement

The figure 4-9 shows that first the defined memory section .EXTRAM is assigned as a portion of 16 Mega Bytes SDRAM and then different sections of code are mapped to this memory portion.

The beamforming algorithm algorithm explained in Chapter 2 is implemented using C language and the image of the target is constructed.

Chapter 5: 3D BEAMFORMING

5.1 Introduction

The 2D microwave imaging through the wall provides the information related to the location of the target. The 2D image shows one horizontal cross section of the target area giving the exact spot in range and cross-range of the object present. It represents the scenario where the viewer is looking from top in the area to be imaged. If multiple such 2D images are cascaded, the 3D image of the object is formed.

Three-dimensional imaging can provide more detail information of the target than two-dimensional image. It can not only provide the information on range and azimuth, but also provide the information of target on height. It also gives information about the target extent in length and width. This additional feature is effective in target classification or identification in enclosed structures or behind the obstacles.

In this chapter, two different approaches have been described following two papers, *"Three-Dimensional Wideband Beamforming for Imaging Through a Single Wall"* by *Fauzia Ahmad, Yimin Zhang, and Moeness G. Amin* using transformation matrix [9] and *"Three-Dimensional Human Imaging for Through-the-Wall Radar"* by *Lingjiang Kong, Guolong Cui, Xiaobo Yang, Jianyu Yang* using permittivity analysis [10]. Then a comparison is carried out between the computational time and the accuracy of the image constructed using these two approaches.

5.2 Data Acquisition for 3D beamforming

As it was the case with 2D imaging, for 3D imaging room to be scanned is divided into pixels. The number of pixels in cross range, downrange and height are 69, 201 and 57. As far as the movement of antenna is concerned, it is placed on the same positioner that was in the case of data acquisition for 2D beamforming. The difference in the 3D scenario is the now the factor oh height is also incorporated. Meaning that previously only horizontal movements of the antenna were to be considered; now vertical movement is also catered for. The vertical antenna positions are denoted by y_{tm}. The scanning process is carried out such that step size for the movement of antenna is controlled by microcontroller. Once a horizontal scan is completed, the antenna is moved one vertical step upwards. And then again scan of this horizontal plane is carried out. The process is repeated until all the planes have been scanned. Data of each horizontal scan is transferred to the computer via VNA; data from all planes is collected and concatenated to form a 3 Dimensional matrix of intensities. This data is then further processed for applying beamforming algorithm.

5.3 Approach using transformation matrix

The concept in this paper builds on the idea used for 2D beamforming. The analysis has been extended using delay and sum beamforming in the presence of a single uniform wall. The third dimension provides valuable information on target heights that can be used for enhancing target discrimination/identification.

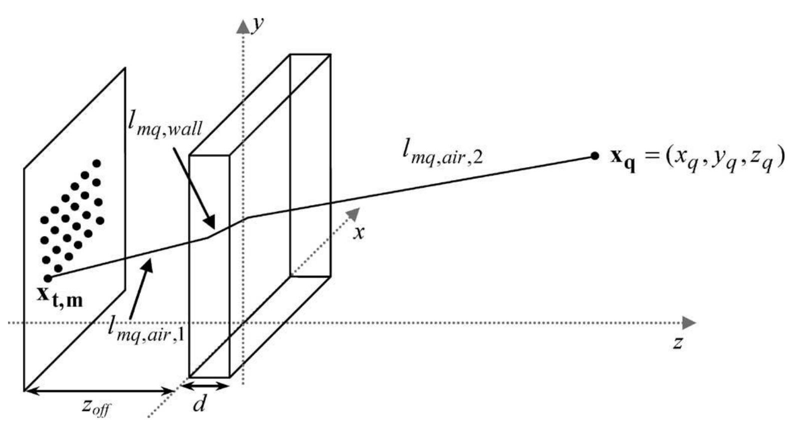

Figure 5-1: Geometry for 3D imaging

The figure 5-1 [9] shows the scene to be imaged which is located beyond the wall along the positive z-axis. The scene is divided into voxels in downrange, crossrange and height, represented by the *z*, *x*, and *y* coordinates, respectively. Voxel can be defined as volume pixel. As with the 2D beamforming case, antenna is placed at a distance of z_{off} from the wall which has a width of *d*. The image is generated using the delay and sum wideband beamforming technique. The grid of x_{tm} shows different antenna locations required to scan the scene and cover all the voxels in target area. At each location, the antenna transmits the signal *s(t)* and the same antenna receives the reflected signal from the target. Then for each antenna location, the focusing delays are calculated and summed for each voxel. Additional weights are applied to control the shape and side lobe structure of the beams.

5.4 Computation of delays

For example the antenna is placed at m_{th} location, so the coordinates of the antenna are (x_{tm}, y_{tm}, z_{off}). For the single point target located at x_p = (x_p, y_p, z_p), the reflected signal at m_{th} location is given by equation 5.1 [9]:

$$r_m(t) = a\left(x_p, y_p\right)s\left(t - \tau_{mp}\right) \tag{5.1}$$

where $a(x_p,y_p)$ is the reflectivity of the target and τ_{mp} is the focusing delay. The propagation and focusing delays are given by equations 5.2 and 5.3 [9].

$$\tau_{mp} = \frac{2 * l_{mp,air,1}}{c} + \frac{2 * l_{mp,wall}}{v} + \frac{2 * l_{mp,air,2}}{c} \tag{5.2}$$

$$v = \frac{c}{\sqrt{\varepsilon}} \tag{5.3}$$

Where the variables are as described before in case of 2D beamforming.

5.5 Dimensional Beamforming

The reflected signal is then summed up for each antenna location, which is given by equation 5.4 [9]:

$$y(t) = \sum_{m=1}^{M} r(x_{tm}, \tau_{mp}) \quad (5.4)$$

In order to cater for the shape of the lobe of the antenna and its varying levels of reflections received from different directivity points, additional weights can be applied to the received signalas given by equation 5.5 [9].

$$y(t) = \sum_{m=1}^{M} w_m\, r(x_{tm}, \tau_{mp}) \quad (5.5)$$

where w_m represent the additional weight. As with the case of 2D beamforming, hamming window in MATLAB is used. Now the lobe will also cover the voxels present in an upper plane. Considering this point, a 2-dimensional hamming window is required to correctly depict the spatial distribution of antenna lobe. Thus a convolution of two such windows is taken which results is a circular pattern as shown in figure 5-2.

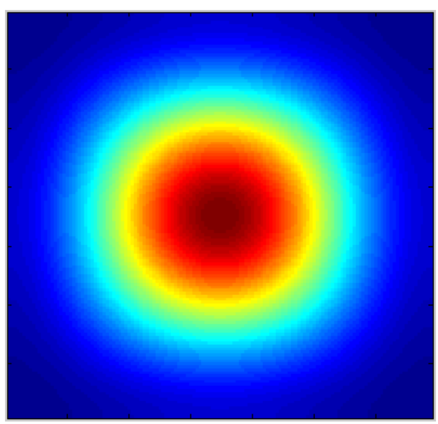

Figure 5-2: 2 Dimensional Hamming Window

The complex amplitude image value $I(x_q)$ corresponding to the *qth* voxel is then obtained by applying a filter, matched to $s(t)$, to $z_q(t)$, and sampling the filtered data, as given in equation 5.6 [9]:

$$I(x_q) = (y(t) * h(t))\,|_{t=0} \qquad (5.6)$$

The traveling distances inside and outside the wall represented in the equation, and subsequently, the focusing delays can be precisely computed, with the knowledge of the wall thickness and its dielectric constant.

5.6 Calculation of angles

Consider the case where the signal first travels from the m_{th} transmitter at x_{tm} to the q_{th} voxel located at x_q, as shown in Figure 5-1. If both x_q and x_{tm} are at the same height, then the problem reduces to the equivalent 2-D problem, as shown in figure 3-1. The expressions for the distances $l_{mq,\mathrm{air},1}$, $l_{mq,\mathrm{wall}}$, and $l_{mq,\mathrm{air},2}$ for the 2D problem as computed before are given by the equations 5.7,5.8 and 5.9 [9]:

$$l_{mp,air,1} = \frac{z_{off}}{\cos\theta_{air}} \qquad (5.7)$$

$$l_{mp,wall} = \frac{d}{\cos\theta_{wall}} \qquad (5.8)$$

$$l_{mp,air,2} = \frac{z_q - d}{\cos\theta_{air}} \qquad (5.9)$$

where θ_{air} is the angle of incidence and θ_{wall} is the angle of refraction, which can be computed by solving the transcendental equation given by equation 5.10 [9]:

$$(x_q - (x_{tm} + z_{off}\tan\theta_{air}))^2 + {z_q}^2 =$$

$$ {l_{mp,wall}}^2 + {l_{mp,air,2}}^2 - 2 l_{mp,wall} l_{mp,air,2} \cos(\pi + \theta_{wall} - \theta_{mq}) \qquad (5.10)$$

These equations represent a very specific case in which the location of the transceivers and the scene voxels lie in the same horizontal plane. The general case is where x_q and x_{tm} lie in different horizontal plane. To find the delays for each voxel, it is required to find the incident angle for each voxel. This necessitates solving the transcendental equation using numerical methods, which now has element of height added to it. This makes the equation very complex to solve and the computational time required to find the angles rises exponentially as the number of elements to be scanned increases. Thus the alternate approach used is that of applying the transformation which is done by using a rotation matrix.

5.7 Rotation matrix

In linear algebra, a rotation matrix is a matrix that is used to perform a rotation in Euclidean space, for example the matrix given in 5.11 [11].

$$R = \begin{bmatrix} \cos\theta & -\sin\theta \\ \sin\theta & \cos\theta \end{bmatrix} \tag{5.11}$$

The matrix Rnrotates points in the xy-Cartesian plane counterclockwise through an angle θ about the origin of the Cartesian coordinate system. To perform the rotation, the position of each point must be represented by a column vector v, containing the coordinates of the point. A rotated vector is obtained by using the matrix multiplication Rv. Usually the transformation is required in two or three dimensions, but rotation matrix for n-dimensional space can also be defined.

Rotation matrices are always square, with real entries. Algebraically, a rotation matrix in n-dimensions is a n × n special orthogonal matrix, i.e. an orthogonal matrix whose determinant is 1, in equation 5.12 [11]:

$$R^T = R^{-1}, \det R = 1 \tag{5.12}$$

For example, for 90^o and 180^o rotation the rotation matrix is depicted in equations 5.13 and 5.14 [11] respectively:

$$R(90^o) = \begin{bmatrix} 0 & -1 \\ 1 & 0 \end{bmatrix} \tag{5.13}$$

$$R(180^o) = \begin{bmatrix} -1 & 0 \\ 0 & -1 \end{bmatrix} \tag{5.14}$$

which gives 90° counterclockwise and 180° rotation in either direction, respectively.

The rotation matrix we have used rotates the 3D scene in x-y plane without making any alterations in z-axis. This transformation has the effect of bringing the m_{th} antenna location and the q_{th} voxel at the same height. The transformation matrix used is given by equation 5.15 and 5.16 [9]:

$$\begin{bmatrix} x'_{tm} \\ y'_{tm} \end{bmatrix} = \begin{bmatrix} \cos\beta & \sin\beta \\ -\sin\beta & \cos\beta \end{bmatrix} \begin{bmatrix} x_{tm} \\ y_{tm} \end{bmatrix} \qquad (5.15)$$

$$\begin{bmatrix} x'_{q} \\ y'_{q} \end{bmatrix} = \begin{bmatrix} \cos\beta & \sin\beta \\ -\sin\beta & \cos\beta \end{bmatrix} \begin{bmatrix} x_{q} \\ y_{q} \end{bmatrix} \qquad (5.16)$$

Such that their y-component has same value i.e. $y'_{tm} = y'_q$. For this condition to be true the angle β is found as in equation 5.17 [9]:

$$\tan\beta = \frac{y_{tm} - y_q}{x_{tm} - x_q} \qquad (5.17)$$

Where β is the vertical component of the angle the *qth* voxel makes with the *mth* antenna location as shown in figure 5-3:

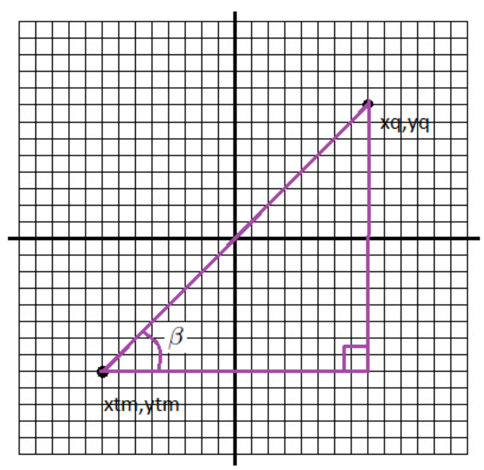

Figure5-3: Angle β between (x_q,y_q) and (x_{tm},y_{tm})

This has the effect as shown in figure 5-4.

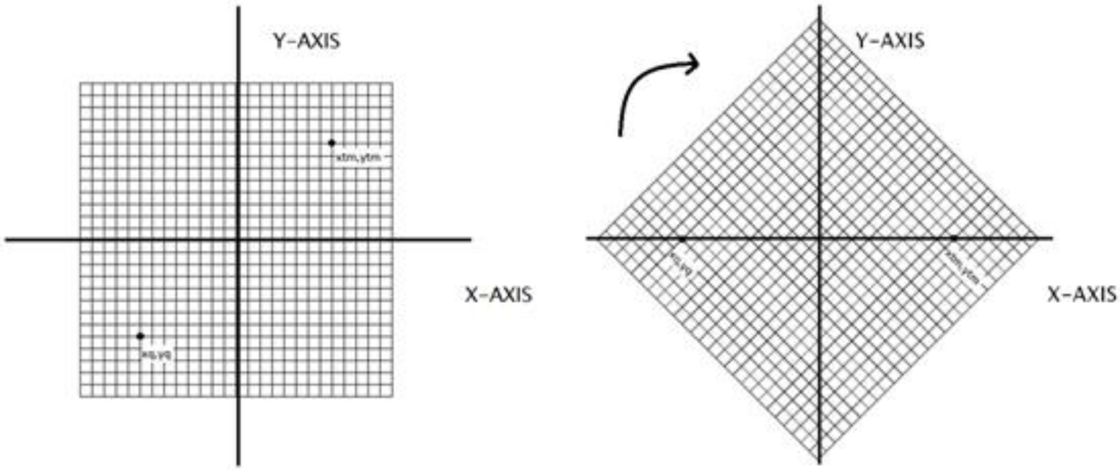

Figure 5-4: The transformation of x-y plane

Now the scenario has reduced to that of a 2D beamforming which has been described before. The transformation preserves the angle of incidence and, as such, does not alter the traveling distance outside and inside the wall between the points x_q and x_{tm}. Thus the same equations to find the angles, and subsequently the delays can be used as were used in 2D beamforming with x_q and x_{tm} replaced by x'_q and x'_{tm} as given in equations 5.18 and 5.19 [9] respectively.

$$x'_q = \cos\beta\, x_q + \sin\beta\, y_q \tag{5.18}$$

$$x'_{tm} = \cos\beta\, x_{tm} + \sin\beta\, y_{tm} \tag{5.19}$$

5.8 Results:

When this beamforming algorithm is applied on a dataset acquired for a human body sitting in the room to be scanned, the following results are obtained as shown in figure 5-5.

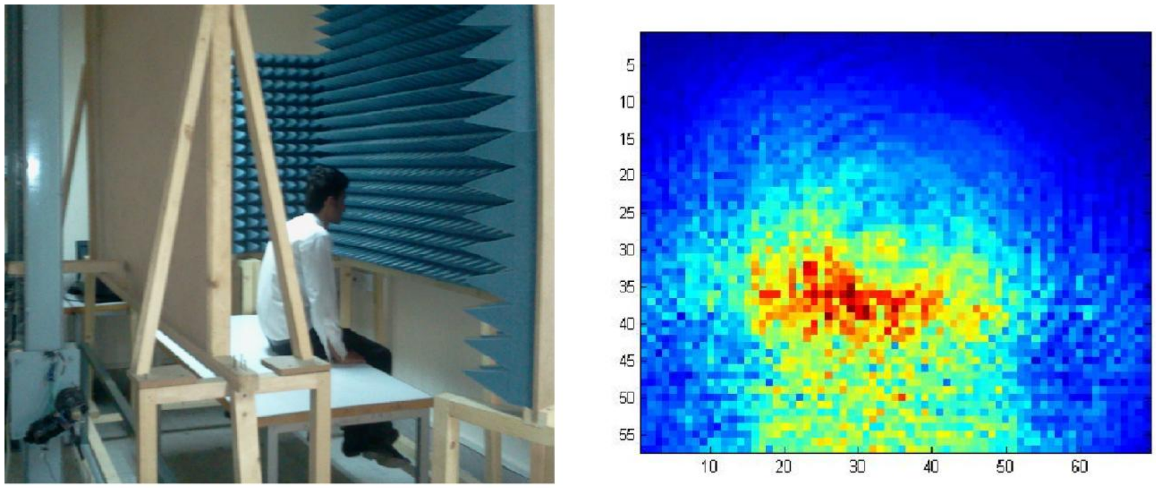

Figure 5-5: Image of a human sitting inside the room beyond the wall

5.9 Approach using permittivity analysis

There may be cases where time is a crucial factor. All the calculations need to be done consuming as little time as possible. Solving the transcendental equation and finding the angles and delays for a new scene may seem to take much of the time. In such scenarios, an approximate method can be used to directly find the refraction point rather than find the solution of complicated transcendental equation as represented in paper "Three-Dimensional Human Imaging for Through-the-Wall Radar".

5.10 Geometry of the scene

Consider the geometry of the scene to be imaged as shown in figure 5-6 [10]:

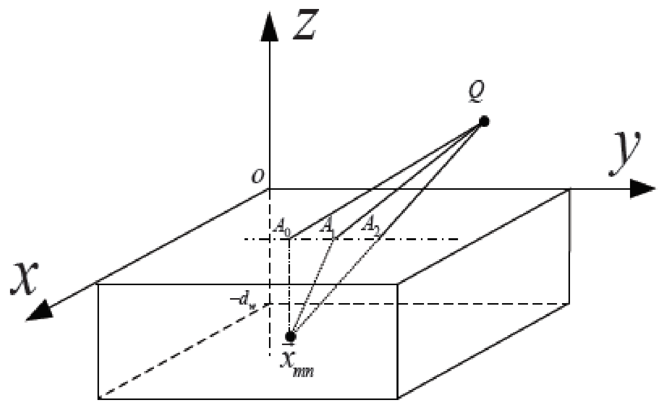

Figure5-6: 3D scene of target area

The antenna is located at x_{tm} where it will transmit the microwave which propagates to the pixel x_q located at location Q along positive z direction. The distance between the antenna and the wall in this is taken to be zero. Thus the propagation delays needs to be found for two regions, within the wall and from wall to the target excluding the delay it would take to travel from antenna to the wall.

5.11 Assumptions regarding permittivity of wall

Suppose the case where the dielectric constant of the wall is equal to 1, which is the dielectric constant of air. For this case, the ray will follow a beeline and will pass without any refraction as it will not meet any boundary with different dielectric constants. It will intersect with the plane z=0 at point A_2. Similarly, when the dielectric constant of the wall is taken to be infinite, the wave will propagate along the normal of the wall and intersect the plane z=0 at point A_0.

In practical situations, the dielectric constant of a wall lies between 1 and infinite. Thus the refraction point of the ray can be inferred to lie between points A_0 and A_2. There is an approximate method to compute the location of the refraction point which intersects the plane z=0 at point A_1. The concept is also used to compute the propagation delay in three-dimensional through the wall imaging.

5.12 Calculation of points of refraction

Suppose the refraction points have the coordinates, A_0 $(x_0,y_0,0)$, A_1 $(x_1,y_1,0)$, A_2 $(x_2,y_2,0)$, the dielectric constant of air is $\varepsilon_1 = 1$ and wall is $\varepsilon_2 = \varepsilon_r$. Thus, the coordinates of the refraction point can be obtained as in equations 5.20 and 5.21 [10]:

$$x_1 = x_0 + \sqrt{\frac{\varepsilon_1}{\varepsilon_2}}(x_2 - x_0) = x_0 + \sqrt{\frac{1}{\varepsilon_r}}(x_2 - x_0) \tag{5.20}$$

$$y_1 = y_0 + \sqrt{\frac{\varepsilon_1}{\varepsilon_2}}(y_2 - y_0) = y_0 + \sqrt{\frac{1}{\varepsilon_r}}(y_2 - y_0) \tag{5.21}$$

Where x_0 and y_0 are given by equations 5.22 and 5.23 [10] respectively

$$x_0 = x_{tm} \tag{5.22}$$

$$y_o = y_{tm} \tag{5.23}$$

Given these equations, the coordinates of A_2 $(x_2,y_2,0)$ can be found by solving the simultaneous equations in 5.24 and 5.25 [10]:

$$\frac{z+d}{\sqrt{(x_{tm}-x)^2+(y_{tm}-y)^2}} = \frac{d}{\sqrt{(x_{tm}-x_2)^2+(y_{tm}-y_2)^2}} \tag{5.24}$$

$$\frac{z+d}{\sqrt{(x_{tm}-x)^2+(y_{tm}-y)^2}} = \frac{z}{\sqrt{(x-x_2)^2+(y-y_2)^2}} \tag{5.25}$$

With the help of these refraction coordinates, the distance a ray travels within and outside the wall can be found out. The distance the ray travels within the wall is given by equation 5.26 [10]:

$$l_{mp,wall} = \sqrt{(x_{tm} - x_1)^2 + (y_{tm} - y_1)^2 + d^2} \tag{5.26}$$

And the propagation distance of the ray in the air is given by equation 5.27 [10]:

$$l_{mp,air} = \sqrt{(x - x_1)^2 + (y - y_1)^2 + z^2} \tag{5.27}$$

5.13 Calculation of propagation delay

With the help of propagation distances within the wall and from wall to the target, the total propagation delay, τ_{mp} which the ray experiences can be expressed as equation 5.28 [10]:

$$\tau_{mp} = 2\,\frac{\sqrt{\varepsilon_r}\,l_{lmp,wall} + l_{mp,air}}{c} \tag{5.28}$$

After finding the delays, the received signal and the composite signal is found in the similar manner as for the other approach which results in target identification.

5.14 Results

Image of a human holding a metallic disc in his hand, standing across the wall is given in figure 5-7.

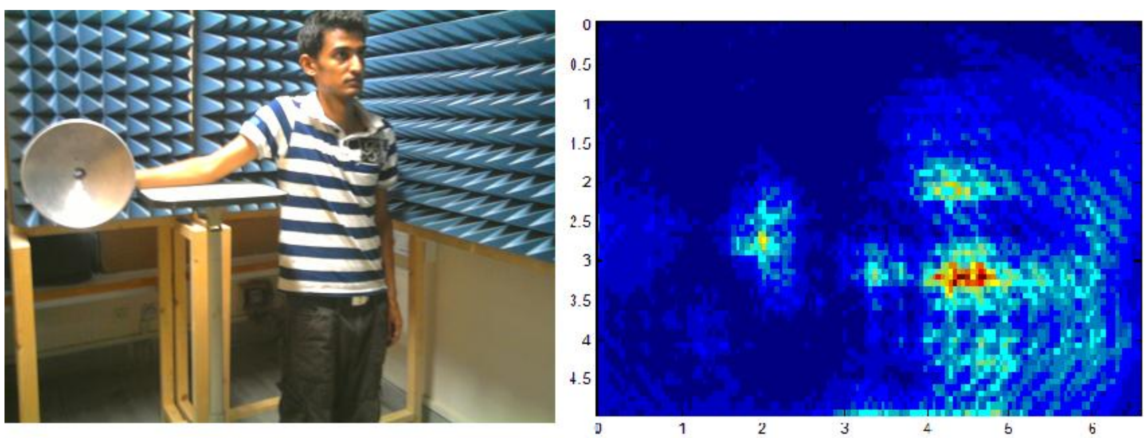

Figure 5-7: Image of a human standing beyond the wall

Image of a parabolic reflector placed inside the room is shown in figure 5-8.

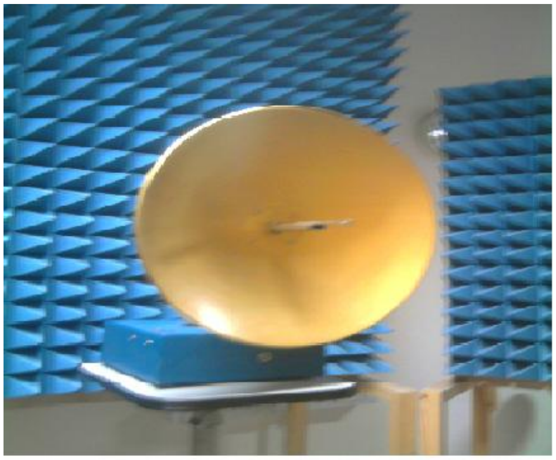

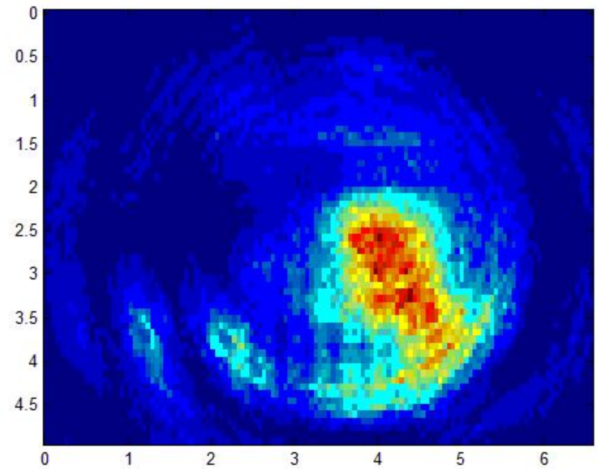

Figure 5-8: Image of a parabolic reflector placed inside the room

5.15 Comparison

For 3-Dimensional beamforming, two different approaches are used, each having its own pros and cons.

In the method using transformation, a rotation transformation is applied to find the incident angles and subsequently the refracted angles for each voxel from each antenna location. This facilitates in finding the distance a beam of microwave travel within and outside the wall and the propagation delay it experiences. This requires finding the angles by solving the transcendental equation using numerical technique. This consumes considerable amount of time. In situations where time is a critical constraint, it may not be suitable to invest time to find the angles. The already calculated angles for any particular scenario cannot be used for different scene due to variations in the dimensions and conditions of the room. Thus, it's a hindrance in making the situation generic. Also, the result obtained using this method is not so accurate. The shape of the object obtained is fuzzy, which provides less clarity and poor identification of the object present in the target area.

In contrast, the approach used in the permittivity analysis uses assumptions on the permittivity of the wall to find out the propagation delays. It considers two cases where the wall has unity and infinite permittivity. Then the point of refraction is found using the geometry of the scene. Using this method, there is no need to find the angles. Thus the calculation and the target detection can be done in lesser time. In addition, the results show that this approach is more efficient in forming the image. The shape of the object is clearer thus making the identification and classification of object easier and efficient.

Therefore, in every respect, the approach of assumptions on permittivity is preferred over the approach using the rotation transformation as it requires less computational time and gives better results.

5.16 Cubism

In 2D beamforming, the antenna locations presented a line array. The antennas need to illuminate one horizontal plane of the target area. When it is extended to 3D beamforming, voxels in multiple horizontal planes are defined to be imaged and antenna locations are needed over a planer array. In result of this, the possible combinations of antenna location and the scene element increases exponentially, in effect increasing the time required to do the computations for 3D imaging.

To avoid this, the concept of cubism is applied to carry out the calculations. To include all the possible combinations of voxels and antenna locations, the 3D matrix of the voxels of scene are cascaded for both vertical and horizontal antenna locations. This can be seen as a planer 2D matrix in which each element contains a 3D matrix. This forms one 3D matrix encapsulating all the data set. Parallel computation can be applied on this set to reduce the time taken for calculation of time delays and thus the intensity present at each voxel as shown in figure 5-9.

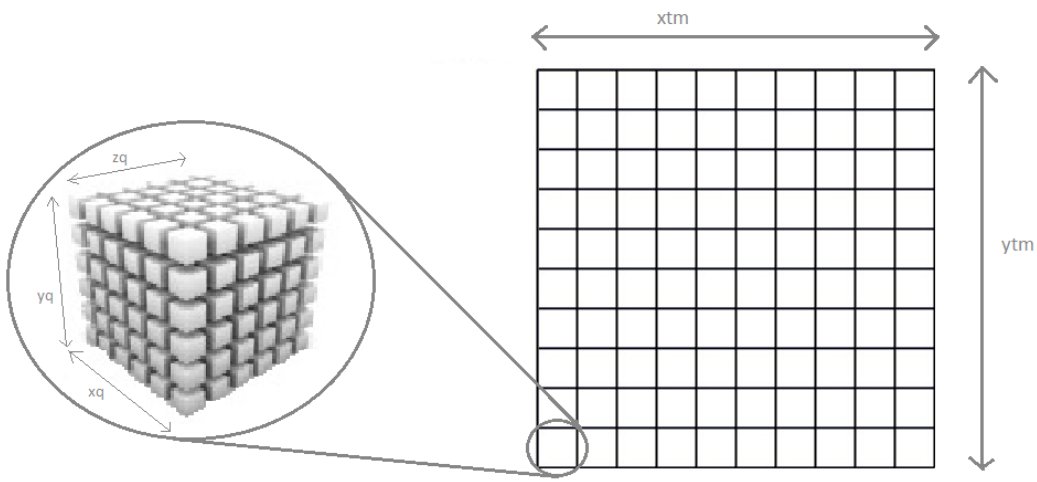

Figure 5-9: Cube encapsulating 3D matrix in 3D beamforming

CHAPTER 6: FUTURE WORK

A number of improvements can be done to this TWMI system. If the use of higher frequency is possible then the system can work for any wall with permittivity greater than that of a wooden wall. In addition multiple targets can be distinguished from each other and moving object detection inside the rooms or buildings is possible. It has its applications in security and defense operations.

A number of image processing techniques can be implemented as well to cater for different scenarios in real time environment. These techniques include FDTD (Finite Difference Time Domain Modeling), Time reversal technique, back scattering and back projection techniques etc.

Algorithm can be composed for image refining and clutter reduction techniques, algorithm should be such that unnecessary reflections are absorbed or ignored without making use of anechoic chamber.

Microwave radar imaging also have its applications in medical imaging, for example for breast cancer detection and imaging of tumor in some parts of body, for such purposes algorithms like Space Time Beamforming can be used.

The concept of TWMI can be extended for mine detection deep inside the ground. This can be achieved by changing the antenna design of through the wall imaging radar to a GPR that is Ground Penetrating Radar. It will be provide a great application in security and defense.

Since our equipment is huge in size, it cannot be taken to field for imaging purposes, there is a need to develop a hardware platform to mount the antenna and that is capable enough to make automatic movements to perform a complete building scan.

Detection and characterization of damages in civil structures is vital for public safety. Since microwaves can penetrate into dielectric materials like concrete, Microwave radar techniques are suitable for in-depth damage assessment of concrete structures in case of some earthquake or other natural disaster.

REFERENCES

[1] Aamna M., Ammar S., Rameez T., Shabeeb S., Naveed I. Rao and Safwat. I, "2D Beamforming for Through-the-Wall Microwave Imaging Applications", *Electrical Engineering Department, MCS, National University of Sciences & Technology,Pakistan*

[2] Aamna M., Ammar S., Rammez T., Shabeeb S., "Through the Wall, Microwave Imaging", *Thesis to The Faculty of Electrical Engineering Department National University of Sciences and Technology, Islamabad*

[3] F. Ahmad and M. Amin, "Noncoherent approach to through-the-wall radar localization", *IEEE Trans. Aerosp. Electron. Syst., vol. 42, no. 4, Oct. 2006, pp. 1405–1419*

[4] E. Engin, B. Ciftcioğlu, M. Özcan and I. Tekin, "A high resolution Ultrawideband Wall Penetrating Radar", *Microwave and Optical Technology Letters*

[5] TMS320C6000 Code Composer studio Tutorial

[6] Rıfat Benveniste, "A Quick Start to Texas Instruments TMS 320C6713 DSK", *Beril Sırmaçek, Cem Ünsalan 21.07.2010*

[7] Rulph Chassaing, "Digital Signal Processing and Application with the 6713 and 6416 DSK"

[8] John Stevenson, "Texas Instruments Code Composer Studio IDE v3 White Paper"

[9] Fauzia Ahmad, Yimin Zhang and Moeness G. Amin, "Three-Dimensional Wideband Beamforming for Imaging Through a Single Wall"

[10] Lingjiang Kong, Guolong Cui, Xiaobo Yang, Jianyu Yang, "Three-Dimensional Human Imaging for Through-the-Wall Radar"

[11] Moeness G. Amin and Fauzia Ahmad, "Wideband Synthetic Aperture Beamforming for Through-the-Wall Imaging"

[12] Jiawei HU, Tao JIANG, Zhengang CUI and Yanli HOU, "Design of UWB Pulses Based on Gaussian Pulse", *Proceedings of the 3rd IEEE Int. Conf. on Nano/Micro Engineered and Molecular Systems January 6-9, 2008, Sanya, China*

[13] AFTANAS, M., “Through wall imaging using M-sequence UWB radar system”, *Thesis to the dissertation examination, Technical University of Kosice, Department of Electronics and Multimedia Communications, Slovak Republic, Feb. 2008.*

[14] F. Ahmad, M. G. Amin, S. A. Kassam, “Synthetic Aperture Beamformer for imaging through a dielectric wall”, *IEEE Trans. on Aerospace and Electronic Systems, Vol. 41, No. 1, pp. 271-283, Jan. 2005.*

[15] R. Dilsavor, W. Ailes, P. Rush, F. Ahmad, W. Keichel, G. Titi, M. Amin, “Experiments on wideband through the wall imaging”, *(Invited Paper), Proc. SPIE Symposium on Defense and Security, Algorithms for Synthetic Aperture Radar Imagery XII Conference, Vol. 5808, pp. 196-209, March-April 2005*.

[16] M. AFTANAS, “Signal Processing Steps for Objects Imaging Through the Wall with UWB Radar”, *SCYR 2009 - 9th Scientific Conference of Young Researchers - FEI TU of Koˇsice*

[17] Chen, F.C., Chew, “Time-Domain Ultra-Wideband Microwave Imaging Radar System”, W.C. *Technology Conference, 1998, IMTC/98, Proceedings*

[18] J. A. McVay, K. M. Yemelyanov, N. Engheta, A. Hoorfar, "Through-the-Wall Imaging and Sensing: an Electromagnetic Perspective," *Proc. SAFE 2007: Workshop on Signal Processing Applications for Public Security and Forensics, April 13-14, Zoughi, R. "Microwave Testing and Evaluation", Amsterdam, The Netherlands: Kluwer, 2000.*

[19] PIC16F872 - 28-Pin, 8-Bit CMOS FLASH Microcontroller - Microchip Technology

[20] C6713 Memory Architecture, Basic Memory Management

ANNEX A: OPERATING MANUAL

EQUIPMENT

The following equipment will be use in order to carry out the whole process of imaging through the wall.

1. Agilent 8417ET VNA for 300kHz-3GHz
2. Calibration kit
3. Quad Ridged Horn Antenna (frequency range 2-3GHz)
4. Antenna positioner
5. A battery with a power rating of 12 volt, 35 watts
6. Coaxial cables
7. RF adapters
8. Computer system having MATLAB v7.0, Code Composer Studio CCS v3.1
9. Radar absorbent Material (RAM)

PROCEDURE

1. Power on the computer work station.
2. Power on VNA
3. Follow the following steps to establish a peer to peer connection between VNA and PC using a LAN cable:
   i. Assign IP address 192.168.0.3 to VNA
   ii. Assign default gateway 0.0.0.0 to VNA
   iii. Assign IP address 192.168.0.1 to PC
   iv. Assign DNS server IP 192.168.0.2 to PC
   v. Restart the PC

4. Attach one end of RF cable to VNA
5. Calibrate the VNA using the steps mentioned below:
    i. Press the CAL button on the VNA screen
    ii. Connect SHORT to other end of RF cable and press MEASURE STANDARD button.
    iii. Connect OPEN to RF cable and press MEASURE STANDARD button
    iv. Finally connect LOAD to RF cable and press MEASURE STANDARD button. Now the VNA is calibrated.

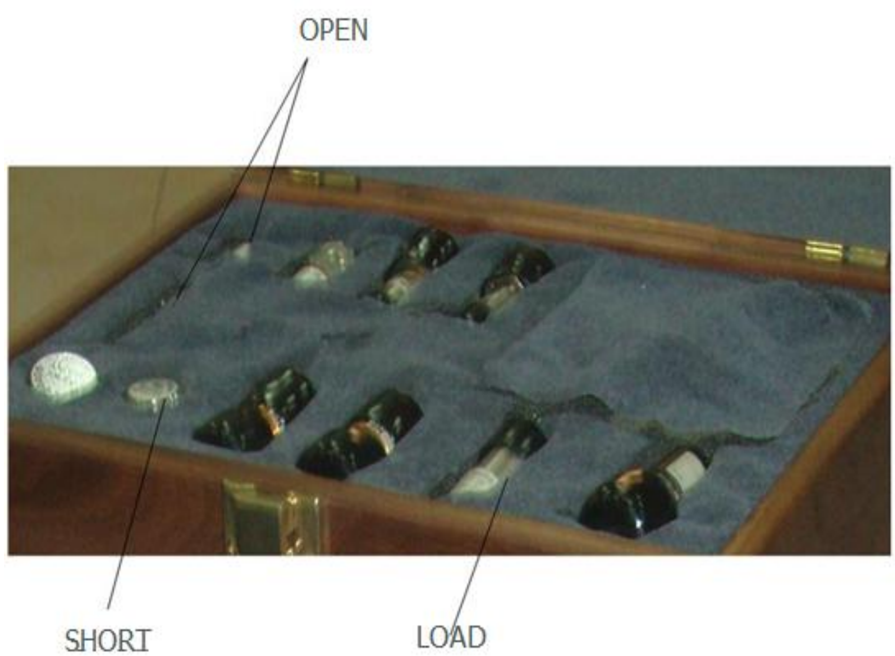

Figure 1: VNA Calibration Kit

6. After calibration the remaining end of RF cable is connected to quad-ridged antenna.
7. Adjust the VNA settings in order to record S11.
    i. Set the power to 0dBm

ii. Set the start frequency range to 2000MHz and stop frequency range to 3000MHz.

iii. Set the number of sweep points to 201.

iv. In the parameter settings, choose the REFLECTION option.

v. Change the display format to SMITH CHART.

Since the Positioner movement control is established using accurate encoders and control is established through microcontrollers. Ensure that whole positioner control is functioning properly, the working of positioner can be verified and debugged manually using Hyper Terminal. It can be accessed as following

Start Button → Accessories → Communication → Hyper Terminal

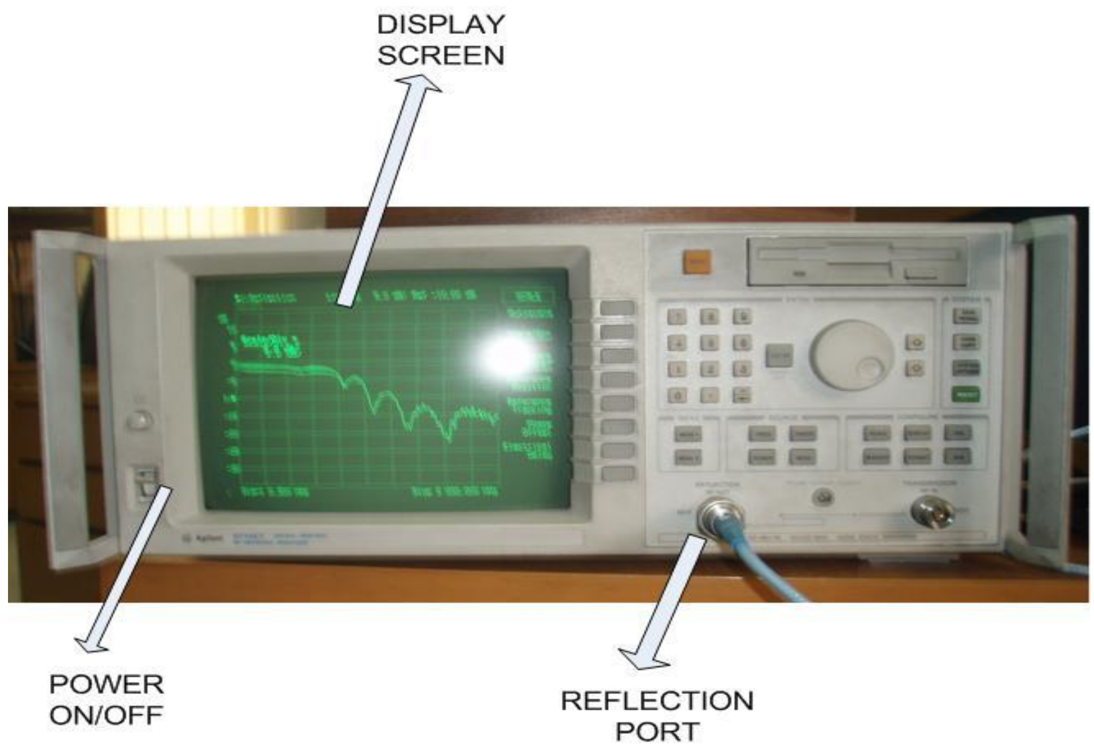

Figure 2: VNA front view

8. Attach serial cable to PC and check the status using MATLAB.
9. Calibrate the room environment and Positioner in range and azimuth.

10. Place a target behind the wall at specific position and mark the location in the room.
11. In MATLAB graphical user interface (GUI), use the manual control option to select the starting position of the scan.
12. Once the antenna is at the starting position, press the automatic scanning option.
13. Steps 11 and 12 are also to be repeated for the same scenario in the absence of target.
14. GUI performs target calibration by subtracting the data obtained in step 13 from the one obtained in step 12.

2D BEAMFORMING:

In order to carry out 2D beamforming on C6713 DSP kit, the following steps should be followed.

1. Connect the DSP kit with computer using JTAG cable
2. Double click 6713DSK Diagnostics icon on the desktop.

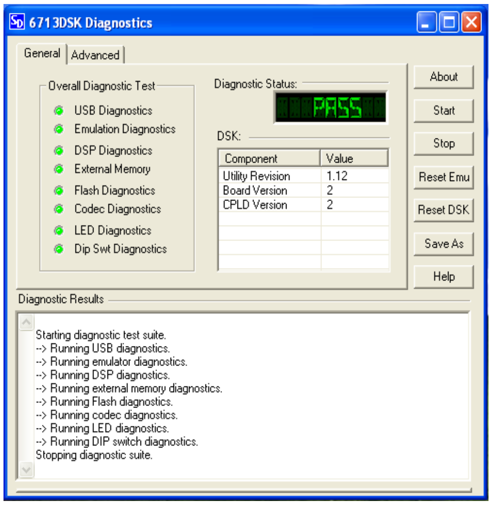

Figure 3: 6713 DSK Diagnostics

3. Press the Start button

4. When PASSED in displayed in the Diagnostic status, close this window
5. Open the 6713DSK CCStudio 3.1, open and build the project
6. From Tools drop down menu, select RTDX and then press Configure, a small widow will appear at the bottom of CCS window, press Configure button, now set value of buffer size to be 65536 and set number of buffers to 6, now check the box Enable RTDX

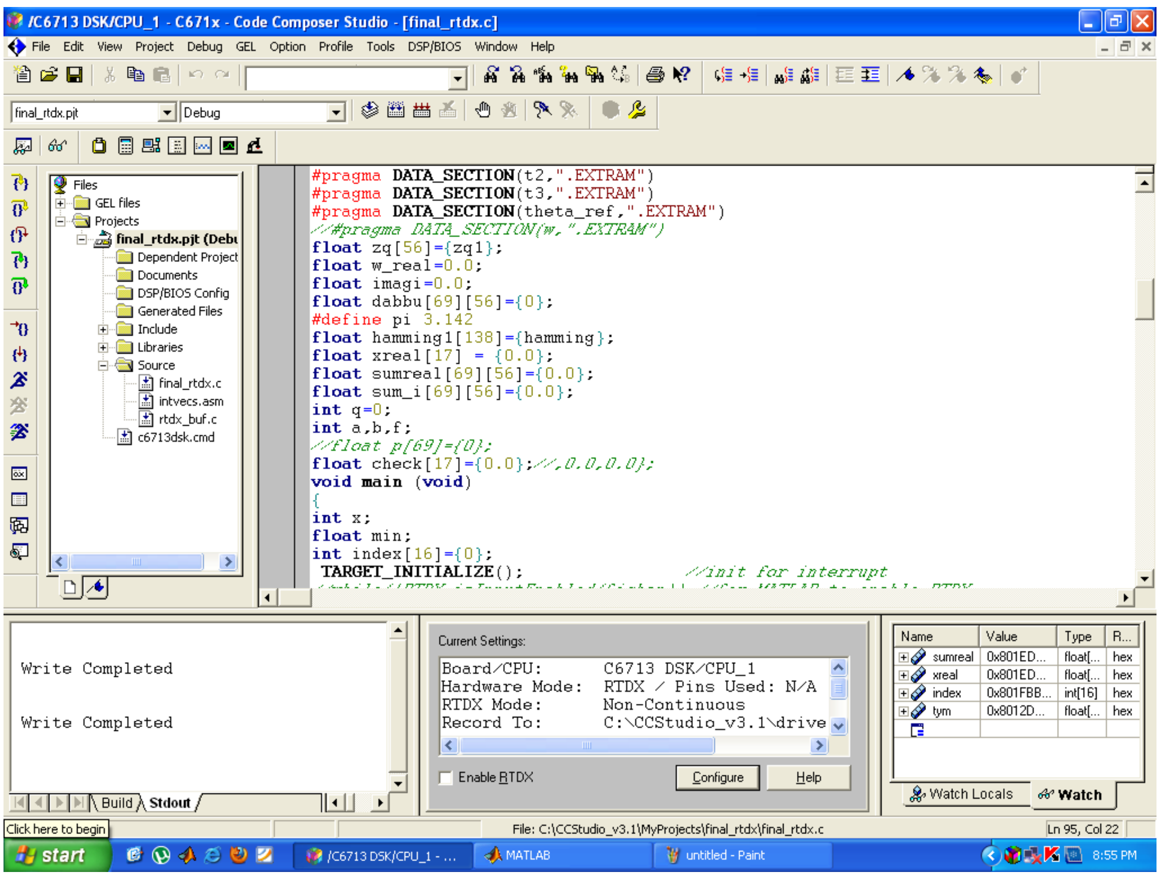

Figure 4: 6713 CCStudio Window

7. Open MATLAB 7.0
8. Click the run button in MATLAB7.0, it will automatically take the data to DSP and after carrying out the processing, results are sent back to MATLAB
9. Result will be displayed in form of an intensity plot.

3D BEAMFORMING

After acquiring the scan data run the 3D Beamforming algorithm. The result will be in form of a 3D matrix.

PRECAUTIONS

1. Do not keep the power level of VNA too high (above 10dBm).
2. Do not touch the tips of microwave absorbers as it can affect their efficiency.
3. Do not bend the RF cable.
4. Turn OFF power of VNA after completing the experiment.